Animal 19 (2025) 101482

Contents lists available at ScienceDirect

Animal
The international journal of animal biosciences

Kinematic changes in dairy cows with induced, unilateral forelimb lameness during straight line walk

A. Leclercq [a,*], K. Ask [a], Y. Mellbin [a], A. Byström [b], M. Söderlind [a], E. Telezhenko [c], C. Bergsten [d], P. Haubro Andersen [a], M. Rhodin [a], E. Hernlund [a]

[a] Department of Animal Biosciences, Swedish University of Agricultural Sciences, Uppsala, Sweden
[b] Department of Applied Animal Science and Welfare, Swedish University of Agricultural Sciences, Uppsala, Sweden
[c] Department of Biosystems and Technology, Swedish University of Agricultural Sciences, Alnarp, Sweden
[d] Department of Clinical Sciences, Swedish University of Agricultural Sciences, Uppsala, Sweden

ARTICLE INFO

Article history:
Received 1 October 2024
Revised 28 February 2025
Accepted 28 February 2025
Available online 13 March 2025

Keywords:
Biomechanics
Bovine
Gait analysis
Inertial measurement unit
Movement asymmetry

ABSTRACT

Early detection of lameness in dairy herds is essential to enable timely treatment of affected animals, thereby avoiding unnecessary costs and animal suffering. Since claw diseases most commonly affect the hind claws, specific kinematic changes in cows with forelimb lameness have not been investigated. However, in-depth knowledge on movement pattern alterations occurring during lameness of varying sources is essential to develop efficient lameness detection tools. In this study, 27 gait analysis trials consisting of > 2 000 strides were collected from 12 clinically sound dairy cows. The cows were equipped with nine body-mounted inertial measurement units (**IMU**s) and contributed with one baseline trial and one or two lameness trials each. A lameness induction method causing increased claw pressure was used to introduce mild, reversible, unilateral forelimb lameness. From the IMU data, 31 limb-and upper body movement parameters, mainly focusing on motion symmetry, were computed for each stride. Baseline and lameness data were compared in linear mixed models, where between-cow variability was accounted for. Twenty-two movement parameters differed between the two conditions ($P \leq 0.05$). Forelimb lameness caused a more pace-like walk; the relative time between hoof-on of both hindlimbs and their respective ipsilateral forelimb decreased by 0.022 and 0.036 (ratio of stride duration), while the relative time between hoof-on of the hindlimb contralateral to the lame forelimb, and the lame forelimb increased by 0.050. The maximum protraction angle of the lame forelimb increased by 1.5°, while the protraction angle of the non-lame forelimb, and the retraction angle of the lame forelimb, decreased by 1.7° and 3.0°. All hindlimb protraction and retraction angles, except the protraction angle of the hindlimb contralateral to the lame forelimb, decreased by 1.2°–1.4°. Following signal decomposition of upper body vertical motion, the largest changes were detected for the head and neck; there were notable increases (0.13 and 0.11) of their first harmonic (asymmetric component) amplitudes, and decreases (0.10 and 0.050) of their second harmonic (symmetric component) amplitudes (relative to the range of motion). Changes in the within-stride differences in the withers' position during limb spread and mid-stance (respectively) were also detected. The vertical range of motion per stride increased for the head, neck, and back, but decreased for the pelvis. Although the investigated parameters hence show promise as lameness indicators, the movement changes occurring with the induced fore claw pain should be confirmed in clinical lameness cases, to ensure usability of the described pattern for early, automated forelimb lameness detection.

Implications

Lameness-causing claw diseases are common in dairy herds. Early detection is important to improve animal welfare. Therefore, systems that can monitor and interpret altered movement patterns of animals are needed. However, until now, almost no research has been performed on movement alterations in cows with forelimb

* Corresponding author.
E-mail address: anna.leclercq@slu.se (A. Leclercq).

https://doi.org/10.1016/j.animal.2025.101482
1751-7311/

Table 1
Definitions for all calculated kinematic parameters, which were calculated on a stride-by-stride basis from the gait analysis trials of all included cows.

Outcome variable	Definition
Re_noninduced_fore	Maximum retraction angle of non-induced forelimb, in degrees
Re_induced_fore	Maximum retraction angle of induced forelimb, in degrees
Pro_noninduced_fore	Maximum protraction angle of non-induced forelimb, in degrees
Pro_induced_fore	Maximum protraction angle of induced forelimb, in degrees
Re_noninduced_side_hind	Maximum retraction angle of hindlimb ipsilateral to non-induced forelimb, in degrees
Re_induced_side_hind	Maximum retraction angle of hindlimb ipsilateral to induced forelimb, in degrees
Pro_noninduced_side_hind	Maximum protraction angle of hindlimb ipsilateral to non-induced forelimb, in degrees
Pro_induced_side_hind	Maximum protraction angle of hindlimb ipsilateral to induced forelimb, in degrees
Poll_ROMz	Vertical range of motion of poll, in millimetres
Neck_ROMz	Vertical range of motion of neck, in millimetres
Withers_ROMz	Vertical range of motion of withers, in millimetres
Back_ROMz	Vertical range of motion of back, in millimetres
Diag_diss (induced limb involvement)	Time between hoof-on of induced forelimb and hoof-on of contralateral hindlimb, as ratio of stride duration
Diag_diss (non-induced limb involvement)	Time between hoof-on of non-induced forelimb and hoof-on of contralateral hindlimb, as ratio of stride duration
Lat_diss (induced limb involvement)	Time between hoof-on of hindlimb ipsilateral to the induced forelimb, and hoof-on of induced forelimb, as ratio of stride duration
Lat_diss (non-induced limb involvement)	Time between hoof-on of hindlimb ipsilateral to the non-induced forelimb, and hoof-on of non-induced forelimb, as ratio of stride duration
TS_ROMz	Vertical range of motion of *tubera sacrale*, in millimetres
Withers_Mindiff	Within-stride difference between local minima of vertical position of withers, in millimetres
Withers_Maxdiff	Within-stride difference between local maxima of vertical position of withers, in millimetres
TS_Mindiff	Within-stride difference between local minima of vertical position of *tubera sacrale*, in millimetres
TS_Maxdiff	Within-stride difference between local maxima of vertical position of *tubera sacrale*, in millimetres
Poll_z_h1_amp	Amplitude of first harmonic of vertical displacement of poll, as ratio (between 0 and 1) of total range of motion
Poll_z_h2_amp	Amplitude of second harmonic of vertical displacement of poll, as ratio (between 0 and 1) of total range of motion
Neck_z_h1_amp	Amplitude of first harmonic of vertical displacement of neck, as ratio (between 0 and 1) of total range of motion
Neck_z_h2_amp	Amplitude of second harmonic of vertical displacement of neck, as ratio (between 0 and 1) of total range of motion
Withers_z_h1_amp	Amplitude of first harmonic of vertical displacement of withers, as ratio (between 0 and 1) of total range of motion
Withers_z_h2_amp	Amplitude of second harmonic of vertical displacement of withers, as ratio (between 0 and 1) of total range of motion
Back_z_h1_amp	Amplitude of first harmonic of vertical displacement of back, as ratio (between 0 and 1) of total range of motion
Back_z_h2_amp	Amplitude of second harmonic of vertical displacement of back, as ratio (between 0 and 1) of total range of motion
TS_z_h1_amp	Amplitude of first harmonic of vertical displacement of *tubera sacrale*, as ratio (between 0 and 1) of total range of motion
TS_z_h2_amp	Amplitude of second harmonic of vertical displacement of *tubera sacrale*, as ratio (between 0 and 1) of total range of motion

lameness. This study investigated this matter and showed that forelimb lameness results in a specific motion pattern which differs from the one seen in hindlimb lameness. This has given a deeper understanding of lameness in cattle and can contribute to the development of automated lameness detection systems, which can help lower lameness prevalence on farms.

Introduction

Lameness in dairy cows is a costly issue (Cha et al., 2010) which threatens animal welfare (Ventura et al., 2015) and leads to premature culling of animals (Jaja and Yanga, 2022). Lameness detection is often done visually by farmers; however, herd-level lameness prevalence is generally heavily underestimated (Leach et al., 2010; Fabian et al., 2014). This is likely due to the fact that visual lameness assessment is inherently subjective and thus prone to observer bias, as well as time–consuming, and hence not performed regularly on farms. As our understanding on movement pattern alterations seen in mild lameness is incomplete, so is knowledge on what to look for in order to spot lame animals at a very early stage. Additionally, so-called "barn blindness" (i.e. when farmers fail to notice issues in their own herd due to habituation) may hamper detection of visibly lame animals (Croyle et al., 2019).

Because of the disadvantages with subjective lameness assessment, considerable efforts have been directed towards developing automatic lameness detection methods (e.g. Alsaaod et al., 2019; Nejati et al., 2023). However, the prevalence of lameness in dairy cows remains high (Thomsen et al., 2023), and mild lameness cases are especially challenging to assess (Winckler and Willen, 2001). To enable timely treatment and thereby prevent the development of chronic claw pathologies with associated production losses (Cha et al., 2010; O'Connor et al., 2023), previous research has shown that it is important to detect claw diseases before they progress to an advanced stage (Leach et al., 2012). Thus, further refinement of lameness detection strategies is warranted.

A large majority of lameness cases in dairy cows stem from foot lesions (Jubb and Malmo, 1991; Fenster et al., 2023). It is also well documented that hindlimbs are more frequently affected (60–80% of cases in different studies) than forelimbs (Jubb and Malmo, 1991; Manske et al., 2002; Fenster et al., 2023). Thus, results from previous research on clinically lame cows are mostly based on data from animals with hindlimb lameness. For the same reason, tools for lameness detection (including both visual lameness scales and objective methods) are likely mostly based on the movement pattern seen during hindlimb lameness, and may hence be less efficient in detecting forelimb lameness. As is well described in horses (Kaneps, 2014; Rhodin et al., 2018; Persson-Sjodin et al., 2023), quadrupedal animals exhibit principally different kinematic changes depending on whether a hindlimb or a forelimb is affected, given the differences in anatomy of the fore- versus hindlimb, their respective relations to the centre of mass, and that the head and neck are closer to the forelimbs than the hindlimbs. Studying the respective kinematics of fore- and hindlimb lameness is therefore essential to give lameness detection tools the ability to be able to better identify the localisation of pathologies.

Today, several systems for objective gait analysis are commercially available and used in equine clinics during lameness investigations (Serra Bragança et al., 2018); in horses, kinetic and kinematic changes associated with lameness are more thoroughly investigated than in bovines (Nejati et al., 2023). These systems most commonly output measures of movement asymmetry based on the inherent properties of symmetrical gaits such as walk and trot. In sound animals, the vertical displacement of the upper body during one stride cycle can, simplistically, be said to form a sinusoid-like curve with two periods (Peham et al., 1996; Keegan et al., 2001; Audigié et al., 2002; Loscher et al., 2016). During lameness, the load redistribution between limbs (where less load is accepted by the painful limb) is reflected by increased between-steps, i.e. within-stride, asymmetry in upper body vertical displacement. This has been demonstrated on several occasions in trotting (Buchner et al., 1996; Keegan et al., 2001; Audigié et al., 2002) and walking (Serra Bragança et al., 2021; Smit et al., 2023) horses. More recently, similar analyses have also proven useful to characterise kinematic changes associated with hindlimb lameness in walking cows (Leclercq et al., 2024). Furthermore, systems for gait analysis can be used to obtain precise temporal and spatial information from all four limbs, and hence, parameters related to limb motion and inter-limb coordination can be obtained (Serra Bragança et al., 2017;2021; Smit et al., 2023) and considered in addition to measures describing upper body kinematics. Thereby, a detailed understanding of the overall movement pattern, where kinematics of numerous anatomical locations are considered, can be acquired. As recent advances in e.g. computer vision are now offering possibilities to monitor multiple body landmarks without the need for sensors or markers (e.g. Anagnostopoulos et al., 2023; Järemo Lawin et al., 2023; Russello et al., 2022; 2024), the addition of more detailed "biological" knowledge could be used to further develop gait analysis systems which can detect subtle, lameness-related changes in the movement pattern as a whole.

By applying such adapted knowledge from the field of equine biomechanics to cattle, we have previously described the kinematics of sound (Tijssen et al., 2021) and hindlimb lame (Leclercq et al., 2024) dairy cows during walking, using a "multi-segment approach" with inertial measurement units (**IMUs**) placed on the limbs and on the upper body to characterise the movement of different anatomical locations simultaneously. In Leclercq et al. (2024), several kinematic parameters showed promise as indicators of mild hindlimb lameness. However, corresponding knowledge is missing for forelimb lameness. Hence, using a similar approach, the current study aimed to characterise kinematic changes associated with forelimb lameness, using a newly developed lameness induction method intended to mimic common claw pathologies.

Material and methods

Animals

The cows used in the study were housed in a freestall system at the Swedish Livestock Research Centre (Swedish University of Agricultural Sciences, Uppsala, Sweden). Subjects were selected based on the following criteria (described in detail in Tijssen et al., 2021): (i) first or second parity, (ii) no obvious conformational deviations, (iii) no findings on a standard clinical examination performed by veterinarians, (iv) no major findings during standard claw examination and trimming (Toussaint-Raven et al., 1989) performed by an experienced claw trimmer, less than 3 months before experimental procedures, and v) udder did not extend lower than the level of the hock joint. Seventeen milk–producing dairy cows (Swedish Red and white: N = 8, Swedish Holstein: N = 9) met these criteria and were thus initially included in the study. Following experimental procedures, the lameness degree was assessed retrospectively using video recordings to ensure absence of visual signs of lameness at baseline (described in detail below).

Experimental procedures

Data were collected at the Swedish Livestock Research Centre (Swedish University of Agricultural Sciences, Uppsala, Sweden). During experiments, inductions of transient hindlimb lameness were also performed along with separate, corresponding baseline trials. Data from hindlimb lameness induction trials and their associated baseline trials are presented in Leclercq et al. (2024). Data from all baseline trials are described in detail in Tijssen et al. (2021).

A 72 m long aisle with dry, diamond-pattern grooved flooring was used for data collection. The goal was to obtain one baseline trial and one to two forelimb lameness induction trials from each cow. Trials were performed for one cow at a time starting with a

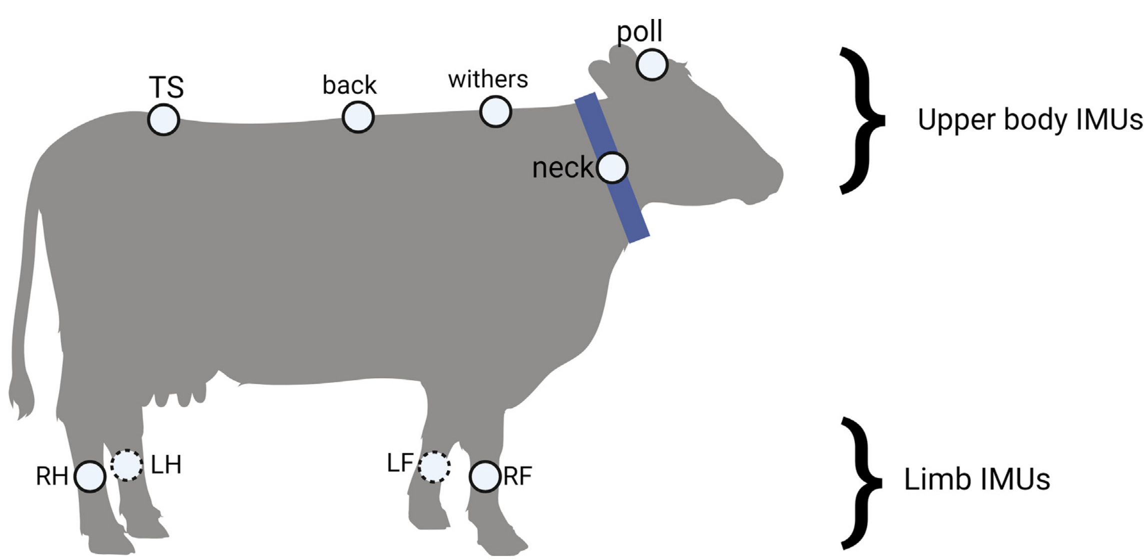

Fig. 1. Placement of the nine IMUs used in the current study on the cow's body. Each white circle represents one IMU. Dashed contour line indicates that the IMU in question is not visible from this view. IMU = inertial measurement unit, TS = *Tubera sacrale*, LF = left front, RF = right front, LH = left hind, RH = right hind. Created in BioRender. Leclercq, A. (2023) BioRender.com/x91k552.

baseline trial, immediately followed by the induction trial(s). Before each induction trial, a "lameness inductor" (described in the section "Lameness induction method") was attached either to the right or the left forelimb. The left or right limb was assigned randomly, from predefined numbers of left and right inductions (thereby achieving equal numbers of left and right inductions). During all trials, the cows were equipped with 11 IMUs which measured high-g and low-g acceleration, as well as angular velocity, in three dimensions (ProMove, Inertia-Technology B.V., Enschede). The IMUs were attached to the following locations: on the poll (poll), on the right side of the neck collar (neck), at the highest point of the withers (withers), on the thoracolumbar junction (back), between the *tubera sacrale* (**TS**), on each *tuber coxae*, and on the lateral aspects of the mid-*metacarpus* and *metatarsus* of all four limbs (left fore = **LF**, right fore = **RF**, left hind = **LH**, right hind = **RH**), respectively (Fig. 1). The four limb IMUs were secured using custom-made touch fastener straps. The remaining IMUs (hereafter referred to as upper body IMUs) were secured using custom-made cases and cyanoacrylate glue, except for the neck IMU which was secured using a custom–made case and adhesive tape. Data from the *tubera coxae* IMUs were not used in the current study, but are presented in Leclercq et al. (2024), where kinematic changes during hindlimb lameness are described.

Sampling frequency was set to 200 Hz, and gyroscope range was set to ± 2 000 deg/s for all IMUs. For the upper body IMUs, the accelerometer range was set to ± 8 g for measuring low-g and ± 100 g for measuring high-g acceleration, and for the limb IMUs, the corresponding ranges were ± 16 g and ± 200 g, respectively. The IMUs were time-synchronised with an accuracy of < 100 ns. Data were transmitted wirelessly from the IMUs to the Inertia gateway, connected to a computer running the software (Inertia Studio version 3.5.2) (Bosch et al., 2018).

After a trial was initiated, a 5-sec period of signal silence (where the cow was standing still) was employed to allow for IMU calibration; the average offset in acceleration and angular velocity, as measured during signal silence, was subtracted from the entire trial (Valenti et al., 2015). Subsequently, the cow was allowed to walk up and down in the measurement aisle one or two times, depending on each cow's motivation. One or two handlers were walking in front of and/or behind the cow and encouraging her to walk, aiming for straight-line, steady-paced walk while minimising handling and interference. During induction trials, the cow's response to the lameness induction was continuously monitored by experienced assessors. If the lameness did not remain stable during the entire trial, the trial in question was discarded. The trial was discontinued if the lameness was deemed too severe, since the aim was to measure mild to moderate lameness, defined as degree 1–2 on a modified version of the Sprecher scale (Sprecher et al., 1997), ranging between 0 and 4 (Coetzee et al., 2014). As described in detail in Coetzee et al. (2014), the different scores are essentially defined as: score 0="stands and walks normally, all feet placed with purpose", score 1="stands with flat back but back arches when walks, gait is slightly abnormal", score 2="stands and walks with arched back, short strides with one or more limbs", score 3="stands and walks with arched back, at least partially weight bearing", score 4="arched back, refuses to bear weight on one limb". After each induction trial, the state of the lameness inductor as well as the claws of the induced limb were inspected. If the inductor was found to be displaced or substantially damaged, the trial in question was discarded. All trials were filmed from the side by a researcher walking 2–3 m from the cow, using a hand-held video camera. Video recordings from all successful trials were assessed retrospectively by two veterinarians (authors A.L. and M.S.), who scored lameness severity for each trial using the modified version of the Sprecher scale (Sprecher et al., 1997; Coetzee et al., 2014).

Lameness induction

For the study, a lameness induction model, previously described in Leclercq et al. (2024), was employed. The aim was to achieve a stable, unilateral, mild to moderate lameness (defined as 1–2 degrees of lameness on a modified Sprecher scale (Sprecher et al., 1997; Coetzee et al., 2014)). Lameness was induced using two different methods, where the first one was intended to mimic discomfort caused by pedal bone displacement, which is commonly seen in association with sole ulcers or sole haemorrhages (Lischer et al., 2002). This method caused lameness by increasing pressure at the caudal third of the sole of the medial fore claw. This

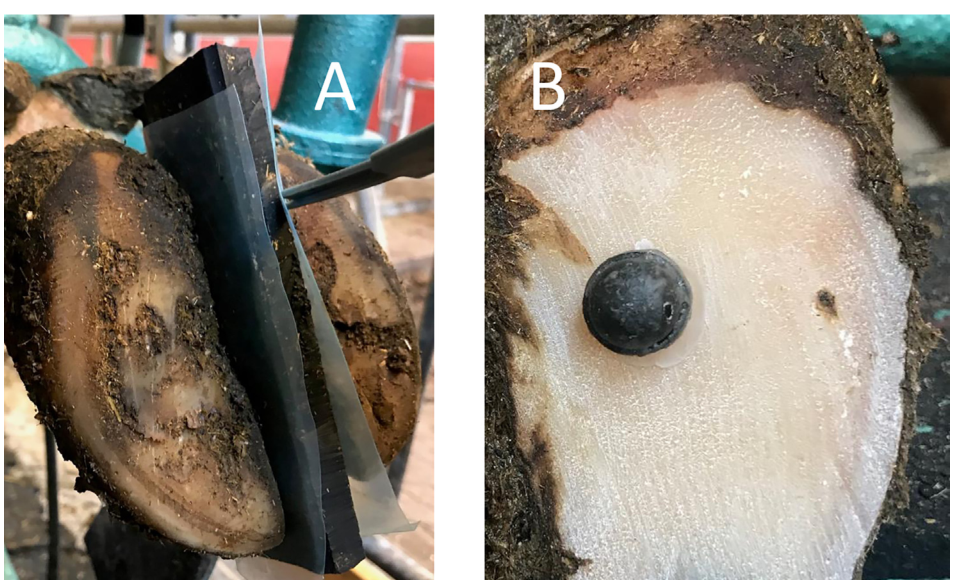

Fig. 2. Images depicting the two lameness induction methods used in this study. A: lameness induction method causing increased pressure to the interdigital space. A cut piece of rubber was placed in the interdigital space, with a plastic film underneath to avoid friction. The rubber piece was secured using elastic bandage and adhesive tape (not shown). B: lameness induction method causing increased pressure to the sole of the medial fore claw. A plastic sphere filled with metal (shown), or a wooden cylinder (not shown) was glued to the caudal third of the cows' medial claw. The lameness inductor was further secured with hoof glue (Equi-Thane Superfast 47140, Vettec, The Netherlands or Bovi-Bond 46120, Vettec, USA), elastic bandage and adhesive tape (not shown).

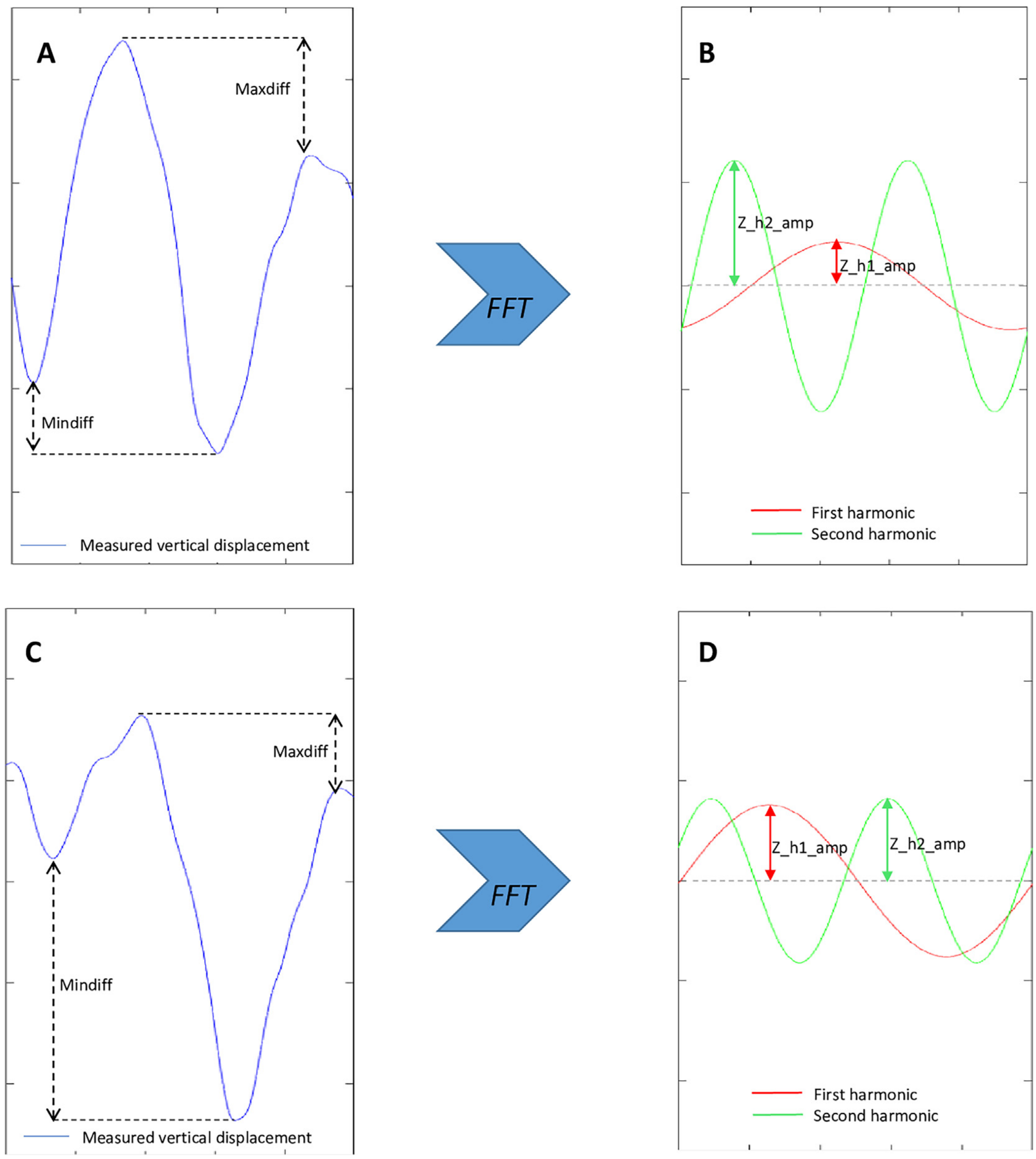

Fig. 3. Visualisation (simplified) of the two methods used for assessment of the cows' within-stride upper body vertical displacement symmetry. A and C: two different examples of vertical displacement of the withers IMU (inertial measurement unit) during one complete walking stride cycle, where a higher degree of within-stride asymmetry is seen in C. Maxdiff is calculated as the within-stride difference between the two local maxima, and Mindiff is calculated as the within-stride difference between the two local minima. B and D show the extracted first two main components (harmonics) of the stride frequency, computed using fast Fourier transform (FFT) of the vertical displacement signals shown in A and C, respectively. The amplitudes of the first and second harmonics of the vertical displacement signal (Z_h1_amp and Z_h2_amp) are indicated. Note the difference in the amplitudes of Z_h1_amp and Z_h2_amp in D compared to B; the amplitude of the first harmonic ("asymmetric component") is higher, and the amplitude of the second harmonic ("symmetric component") is lower, which reflects the high degree of within-stride asymmetry seen in the original vertical displacement signal (C).

location was used to ensure an efficient lameness induction; more weight is carried on the medial compared to the lateral claw in the forelimbs, whereas it is the other way around for the hindlimbs (Van der Tol et al., 2003). Lameness induction was achieved using a wooden cylinder or a plastic nut protection cap (Stabilit M8/M6, 5552007/5552006, BAHAG AG, Germany), hereafter referred to as "plastic sphere". The plastic sphere was filled with chemical metal (Chemical metal plastic padding, Pattex, Sweden) and left to harden before being attached to the claw. Before attachment of the plastic sphere/wooden cylinder, the superficial layer of the claw in question was trimmed. The plastic sphere/wooden cylinder was then glued to the claw using cyanoacrylate glue and hoof glue (Equi-Thane Superfast 47140, Vettec, The Netherlands or Bovi-Bond 46120, Vettec, USA), and secured with adhesive bandage and tape. The second method was intended to mimic discomfort experienced during digital dermatitis (Thomas et al., 2022), interdigital phlegmon (Van Metre, 2017) or interdigital hyperplasia (Cramer and Solano, 2023). This method caused lameness by increasing pressure to the interdigital space, using a rectangular piece of rubber (length: 150 mm, height: 30–50 cm, thickness: 18 mm), which was placed in this location. The rubber piece filled the whole interdigital cleft and protruded 22–25 mm distal to the sole, thus causing pressure during stance of the limb in question. The edge of the rubber piece which was in contact with the interdigital cleft was rounded, and covered by a plastic film to avoid skin damage due to pressure peaks and friction. The foot was then wrapped in elastic bandage and adhesive tape to keep the rubber piece in place. The size of the lameness inductor (i.e. the wooden cylinder/plastic sphere/rubber piece) was adjusted as needed, based on individual responses and hoof size, to achieve the desired degree of lameness (Fig. 2).

Data processing

Data from all included trials were imported to Matlab (version R2023a, the MathWorks Inc, Natick, United States). Segments of IMU data, where the cow was walking normally in a straight line without interference, were selected for analysis using generated plots. These plots indicated stance phases of each hoof relative to time, together with video recordings which were time synchronised with the plots (described in more detail in Leclercq et al., 2024; Tijssen et al., 2021).

The selected IMU data were then preprocessed as described previously (Bosch et al., 2018). The acceleration was rotated from a local to a global reference frame and the Z-axis was aligned with gravity (Bosch et al., 2018). The orientation of each IMU was calculated based on the quaternion-based complementary filter (Valenti et al., 2015), also detailed in Bosch et al. (2018). Vertical displacement of the upper body IMUs was calculated by double integrating the accelerometer signal as described in (Pfau et al., 2005). Hoof-on and hoof-off moments were detected from the limb IMUs using existing algorithms (Serra Bragança et al., 2017), and the selected data were split into strides based on hoof-on moments of the left hindlimb. Stride duration (i.e. the duration between two consecutive hoof-on moments of the left hindlimb) was calculated for each stride.

Upper body parameters

Two approaches (Fig. 3) were employed to assess upper body vertical displacement symmetry. First, within-stride differences between local minima and maxima (respectively) of the vertical displacement signal were calculated. This was only done for the withers and TS IMUs, since these calculations require the presence of two relatively clear maxima and minima per stride, which is often not the case for poll, neck and back IMU signals from walking cows (Tijssen et al., 2021), especially if lame (Leclercq et al., 2024). Hence, within-stride differences (in millimetres) between the two local minima (**Mindiff**) and maxima (**Maxdiff**) were calculated for each stride as described in more detail in Leclercq et al. (2024) and defined as withers_Mindiff, withers_Maxdiff, TS_Mindiff, and TS_Maxdiff. For these parameters, values of higher magnitude indicate higher asymmetry, and values closer to zero indicate lower asymmetry. The total vertical (z-direction) range of motion (**ROMz**) per stride in millimetres was also calculated for all upper body IMUs, and defined as poll_ROMz, neck_ROMz, withers_ROMz, back_ROMz, and TS_ROMz. For visualisation purposes, stride-normalised plots displaying the upper body vertical displacement were made for each trial and upper body IMU as previously described (Leclercq et al., 2024).

Second, a signal decomposition method was used to compute the amplitudes of the vertical displacement signal's first and second harmonic. This was done for all upper– body IMUs on a stride-by-stride basis using fast Fourier transform, as described by Roepstorff et al. (2021). Harmonics are basically sine waves where the first harmonic oscillates with the stride frequency, the second harmonic oscillates with 2x stride frequency, etc. Due to the nature of symmetrical gaits, where the upper body midline normally oscillates up and down twice per stride cycle, the first and second harmonic are expected to explain the majority of the signal. Hence, only the first two harmonics of the stride frequency were analysed. The first harmonic can be described as the "asymmetric component", and the second harmonic as the "symmetric component" (Keegan et al., 2001; Audigié et al., 2002; Leclercq et al., 2024). An increase of the first harmonic relative to the second harmonic indicates increased asymmetry, and vice versa. The amplitudes (**amp**) of the first (**h1**) and second (**h2**) harmonics of vertical displacement of the upper body IMUs were calculated for each stride, as a ratio between 0 and 1 of the total range of motion, and defined accordingly as: poll_z_h1_amp, poll_z_h2_amp, neck_z_h1_amp, neck_z_h2_amp, withers_z_h1_amp, withers_z_h2_amp, back_z_h1_amp, back_z_h2_amp, TS_z_h1_amp, and TS_z_h2_amp, respectively.

Limb parameters

Using the determined sagittal orientation of the limb IMUs (Bosch et al., 2018), the stride-segmented limb angle curves were aligned, and maximum protraction (**pro**) and retraction (**re**) angles of the metatarsal and metacarpal segments were calculated for each stride. Forward extension (i.e. protraction) of the distal limb was defined as positive direction, and backward extension (i.e. retraction) was defined as negative direction.

Next, temporal limb parameters were calculated on a stride-by-stride basis. Diagonal dissociation (**diag_diss**) was calculated as the time between the hoof-on of the left/right forelimb, and subsequent hoof-on of the contralateral (right/left) hindlimb, as a ratio of the total stride duration. Lateral dissociation (**lat_diss**) was calculated as the time between hoof-on of the left/right hindlimb, and subsequent hoof-on of the ipsilateral (left/right) forelimb, as a ratio of the total stride duration. Hence, in a completely uniform walking stride where each hoof-on moment is equally spaced in time, each of these temporal parameters would be equal to 0.25. As the temporal parameters are expressed as a ratio of the total stride duration, their sum is always 1 for each stride; if one ratio decreases, it is implied that at least one other ratio has increased.

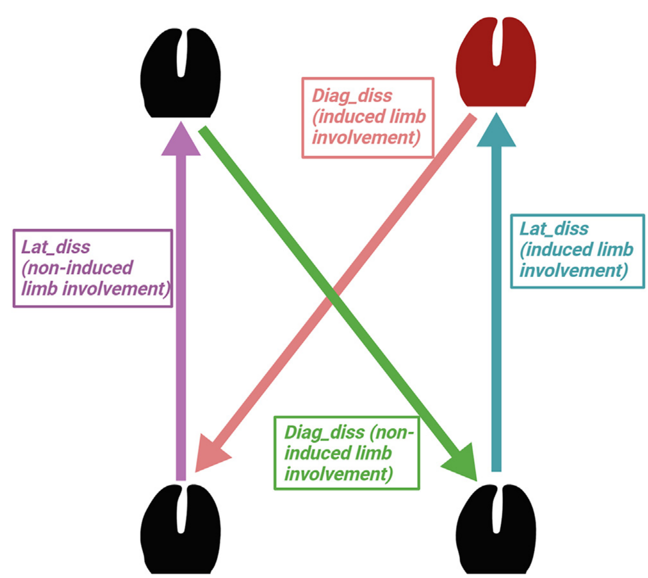

Fig. 4. Schematic representation of temporal limb parameters, after mirroring procedures. All four claw-on moments are represented by a cow's claw silhouette, where the claw subjected to lameness induction (i.e. right fore in this example) is indicated by red colouring. The footfall sequence is indicated (1–4). The time between claw-on of the induced limb and its contralateral hindlimb (indicated by the pink arrow and label) is defined as diag_diss (induced limb involvement). The time between claw-on of the hind limb contralateral to the induced forelimb and its ipsilateral forelimb (indicated by the purple arrow and label) is defined as lat_diss (non-induced limb involvement). The time between claw-on of the non-induced forelimb and its contralateral hindlimb (indicated by the green arrow and label) is defined as diag_diss (non-induced limb involvement). The time between claw-on of the hindlimb ipsilateral to the induced forelimb, and the induced forelimb (indicated by the blue arrow and label) is defined as lat_diss (induced limb involvement). Created in BioRender. Leclercq et al. (2024). BioRender.com/u67i526.

Validation and quality assurance

Validation procedures, previously described in detail in Leclercq et al. (2024) were carried out to ensure soundness of calculated parameters. For the withers and TS IMUs, vertical displacement was plotted against time, with automatically identified local minima and maxima displayed for validation. In cases where extrema were incorrectly detected (i.e. identified to other locations on the signal than local maxima/minima), calculated withers_Mindiff, withers_Maxdiff, TS_Mindiff, and TS_Maxdiff values were excluded from the strides in question. For the limb IMUs, the protraction- and retraction angles of all four limbs were plotted against time for the selected data. Automatically identified hoof-on moments of both hindlimbs were displayed. Signals were inspected visually, and when disturbances (deemed to have occurred because of instrumentation errors) were identified, they were handled according to the following principles.

LH IMU disturbance: exclusion of all data (both limb and upper body parameters) from the strides in question, as this IMU was used for splitting the data into strides. LF/RF IMU disturbance: exclusion of forelimb maximum protraction- and retraction angles (pro_and re_) and temporal parameters (diag_diss and lat_diss) from the strides in question. RH IMU disturbance: exclusion of hindlimb maximum protraction- and retraction angles (pro_and re_) and temporal parameters (lat_diss and diag_diss) from the strides in question.

Standardisation of data

Before statistical analysis, data were standardised with regard to the induced limb, i.e., the calculated variables were adjusted to refer to induced and non-induced limbs instead of left and right. To account for the fact that some cows displayed baseline asymmetries, the same adjustments were applied both to the induction measurements and their corresponding baseline measurements. For the temporal parameters and maximum protraction and retraction angles, this was done by simply re-labelling the variables for each cow depending on which forelimb was subjected to lameness induction. The adjusted labels are listed in Table 1, and diag_diss (induced/non-induced limb involvement)" and "lat diss (induced/non-induced limb involvement") are also illustrated in Fig. 4. For Mindiff and Maxdiff parameters, (Table 1) values from cows with a left forelimb induction were multiplied by −1. After this procedure, these parameters can be interpreted in the same way for all cows, namely: a positive withers_Maxdiff indicates that the withers attained a higher position in midstance of the non-induced forelimb, and a negative withers_Maxdiff indicates the opposite, i.e. a higher position in midstance of the induced limb. A positive withers_Mindiff indicates a lower position in early stance of the non-induced limb (i.e. during late stance/retraction of the induced limb), while a negative withers_Mindiff indicates the opposite. A positive TS_Maxdiff indicates that the TS attained a higher position in midstance of the hindlimb ipsilateral to the non-induced forelimb, while a negative TS_Maxdiff indicates the opposite. A positive TS_Mindiff indicates a lower position during early stance of the hindlimb ipsilateral to the induced forelimb, while a negative TS_Mindiff indicates the opposite.

Statistical analysis of data

Statistical analysis was performed on stride-by-stride data in R version 4.3.2 (R Core Team, 2023), in the R Studio interface, version 2023.09.01 (Posit Team 2023). Differences between the baseline and lameness conditions were assessed in linear mixed models (package: "lme4", Bates et al., 2015). A total of 31 models were created, one for each of the continuous outcome variables detailed in Table 1. Cow and trial within cow were included as random effects in all models. Explanatory variables were condition (i.e. baseline or lameness) as a categorical, fixed effect and stride duration as a continuous, fixed effect. Stride duration was included as a proxy to adjust for speed, which is known to influence kinematic parameters (Walker et al., 2010). The interaction between stride duration and condition was then tested in all models and kept if statistically significant. Before inclusion of stride duration in the models, the effect of condition on stride duration was tested in a separate model with stride duration as a continuous outcome variable, condition as a categorical fixed effect, and cow as well as trial within cow as random effects. Homoscedasticity and normality of residuals were assessed using quantile–quantile-plots and residual plots. Poll_ROMz, neck_ROMz, withers_ROMz, back_ROMz and TS_ROMz were log−transformed (natural logarithm), and TS_z_h1_amp was square root transformed to achieve normality and homoscedasticity of residuals. For the remaining outcome variables, original data were used as residuals were approximately normally distributed and no severe signs of heteroscedasticity were present.

P-values for stride duration and interaction between stride duration and condition were computed in type III ANOVAs (package: "car", function Anova; Fox and Weisberg, 2019) with Kenward-Roger degrees of freedom (package: "pbkrtest", Halekoh

Table 2
Overview of performed gait analysis trials. Induced limb is indicated for each cow; LF = left front and RF = right front. The size of the lameness inductor (given in cm for each trial) was adjusted as needed to achieve the desired lameness degree for each individual cow. Reasons for exclusion of trials are given as footnotes. Examples of video excerpts from all three trials of cow 17 are shown in Supplementary Material S1.

	Baseline trial	Induction trial 1	Induction trial 2	
Cow ID	Lameness degree	Lameness degree/lameness inductor	Lameness degree/lameness inductor	Induced limb
3	0	1/rubber piece 5 cm	Not performed	LF
4	0	1/rubber piece 5 cm[1]	1/rubber piece 5 cm	RF
5	0	1/rubber piece 5 cm	1/plastic sphere 1.5 cm[1]	RF
6	0	1/rubber piece 5 cm	1/plastic sphere 1 cm	LF
7	0[2]	-/wooden cylinder 1.1 × 1 cm[3]	Not performed	RF
8	0	-/rubber piece 5 cm[4]	2/rubber piece 3 cm	LF
9	0	1/rubber piece 4 cm	2/rubber piece 5 cm	RF
11	0	1/rubber piece 5 cm	Not performed	LF
12	0	2/rubber piece 5 cm	Not performed	RF
13	0	-/rubber piece 5 cm[3]	2/plastic sphere 1.5 cm	RF
14	0[2]	-/wooden cylinder 1.1 × 1 cm[1]	Not performed	LF
15	0	1/rubber piece 5 cm	Not performed	LF
16	0	1/rubber piece 5 cm	Not performed	LF
17	0	1/rubber piece 4 cm	1/rubber piece 5 cm	RF

[1] Issues with technical equipment during trial/handling issues.
[2] Baseline trial excluded due to no successful induction trial for the cow in question.
[3] Unstable lameness (decreasing or disappearing lameness) as judged by visual evaluation during the trial.
[4] Interrupted after few strides due to lameness degree >2.

Table 3
Linear mixed model analysis results, performed on stride-by-stride data from the gait analysis trials for the 12 included cows, summarised. Model estimates with SEs, contrast *P*-values, regression slope estimates, and RSDs are given in separate columns. Identical slope estimates in both conditions (baseline and lameness) indicates no significant interaction between stride duration and condition (i.e. the interaction term was not included in the model). Non-identical slope estimates in the baseline and lameness condition indicate that stride duration had different effects on the outcome parameters depending on the condition. A positive slope indicates an increase in the outcome parameter with increasing stride duration, and a negative slope estimate indicates a decrease in the outcome parameter with increasing stride duration. For outcome variables which were transformed before analysis (poll_ROMz, neck_ROMz, Withers_ROMz, Back_ROMz, TS_ROMz, and TS_z_h1_amp), estimates are given on the transformed scale. The transformation which was applied is indicated in left column; "log trans" indicates that a natural logarithm transformation was applied, while "sqrt trans" indicates that a square root transformation was used. See Table 1 for abbreviation definitions.

Outcome variable	Baseline estimate [1] (SE)	Lameness estimate [1] (SE)	Contrast *P*-value	Slope estimate; baseline	Slope estimate; lameness	RSD
Re_noninduced_fore	−47.5 (1.35)	−47.7 (1.34)	0.78	4.59	10.97	2.75
Re_induced_fore	−48.5 (1.35)	−45.5 (1.30)	0.029	8.18	5.54	3.06
Pro_noninduced_fore	26.1 (0.49)	24.4 (0.48)	<0.001	−0.10	−2.06	1.48
Pro_induced_fore	25.8 (0.58)	27.3 (0.57)	0.0026	0.13	1.97	1.65
Re_noninduced_side_hind	−30.3 (0.87)	−28.9 (0.87)	<0.001	2.83	7.51	1.95
Re_induced_side_hind	−30.7 (0.82)	−29.4 (0.82)	0.0030	2.57	4.21	2.34
Pro_noninduced_side_hind	25.0 (0.44)	24.6 (0.44)	0.15	−3.79	−3.79	1.74
Pro_induced_side_hind	24.5 (0.61)	23.3 (0.60)	0.0074	−3.52	−5.88	1.99
Diag_diss (induced limb involvement)	0.266 (0.0067)	0.272 (0.0065)	0.26	−0.043	−0.0071	0.0311
Diag_diss (non-induced limb involvement)	0.255 (0.0091)	0.305 (0.0090)	<0.001	−0.012	−0.012	0.0328
Lat_diss (induced limb involvement)	0.247 (0.0082)	0.225 (0.0078)	0.030	0.011	0.011	0.0328
Lat_diss (non-induced limb involvement)	0.233 (0.0070)	0.197 (0.0068)	<0.001	0.040	0.011	0.0307
Poll_ROMz (log trans)	4.14 (0.094)	4.57 (0.091)	<0.001	0.34	0.34	0.43
Neck_ROMz (log trans)	3.93 (0.088)	4.34 (0.084)	<0.001	0.68	0.68	0.40
Withers_ROMz (log trans)	3.69 (0.054)	3.68 (0.054)	0.77	−0.10	−0.26	0.18
Back_ROMz (log trans)	3.04 (0.074)	3.26 (0.072)	0.0018	0.10	0.10	0.23
TS_ROMz (log trans)	3.72 (0.068)	3.67 (0.068)	0.043	−0.34	−0.34	0.17
Withers_Mindiff	5.43 (3.540)	−3.40 (3.360)	0.036	−4.26	−12.24	9.29
Withers_Maxdiff	−2.41 (1.440)	1.58 (1.400)	0.0046	−0.41	−0.41	7.15
TS_Mindiff	−1.09 (2.380)	−0.33 (2.300)	0.73	−5.27	−5.27	8.63
TS_Maxdiff	0.34 (0.962)	−0.82 (0.923)	0.26	1.14	9.33	6.09
Poll_z_h1_amp	0.44 (0.030)	0.57 (0.028)	0.0020	0.18	−0.082	0.14
Poll_z_h2_amp	0.37 (0.031)	0.27 (0.030)	0.0065	−0.38	−0.044	0.11
Neck_z_h1_amp	0.40 (0.026)	0.51 (0.024)	0.0071	0.038	−0.19	0.13
Neck_z_h2_amp	0.33 (0.022)	0.28 (0.021)	0.031	−0.095	0.15	0.10
Withers_z_h1_amp	0.22 (0.021)	0.26 (0.020)	0.087	0.11	0.11	0.079
Withers_z_h2_amp	0.51 (0.017)	0.47 (0.016)	0.0036	−0.25	−0.25	0.073
Back_z_h1_amp	0.25 (0.016)	0.26 (0.015)	0.46	0.042	0.042	0.092
Back_z_h2_amp	0.40 (0.019)	0.44 (0.018)	0.015	−0.14	−0.14	0.087
TS_z_h1_amp (sqrt trans)	0.42 (0.017)	0.45 (0.090)	0.16	0.20	0.09	0.11
TS_z_h2_amp	0.64 (0.018)	0.58 (0.017)	0.0081	−0.38	−0.38	0.099

[1] Estimated marginal mean.

and Højsgaard, 2014) using Wald F-tests (package: "lmerTest", Kuznetsova et al., 2017). Estimated marginal means and contrast *P*-values for comparison between conditions (baseline and lameness) were computed at grand mean stride duration using the function "emmeans" (package: "emmeans", Lenth, 2023). Slope estimates for interactions were computed using the function "emtrends" (package: "emmeans", Lenth, 2023). Alpha was set to 0.05 for all analyses.

Results

Of the 17 selected cows, three were excluded from the study; one due to handling issues (cow 10); one due to a small indentation in the claw horn following hindlimb lameness inductions (cow 1, described in Leclercq et al. (2024)); and one retrospectively due to lameness already at baseline (cow 2). For the remaining 14 cows, a total of 35 trials were recorded, including 14 baseline trials and 21 lameness induction trials. Out of these, eight trials were excluded for reasons detailed in Table 2. Thus, a total of 27 trials from 12 cows, where each cow contributed with one baseline trial and one or two lameness induction trial(s), were included in the study. Examples of video excerpts from the baseline trial, and both induction trials, of one same cow are shown in Supplementary Material S1. For the included lameness induction trials, the subjectively assigned lameness score was 1/4 (in 11 instances) or 2/4 (in four instances). These 27 trials initially consisted of 2 574 complete stride cycles, ranging between 27 and 142 stride cycles per trial.

For one of the cows (cow 15), recording issues in raw data from the poll IMU were detected, and thus data from this IMU were excluded completely from further analyses for the trials in question. All other trials had at least partially usable data for all IMUs. Artefacts in IMU data were detected in 217 stride cycles for the LH IMU, 42 stride cycles for the RH IMU, and 53 stride cycles for the RF and/or LF IMU. After the exclusion of data for affected variables, data from a total of 2051–2357 stride cycles (depending on parameter) were finally included in statistical analyses. See Supplementary Table S1 for a detailed overview of the number of included strides per parameter.

Linear mixed model analysis

The linear mixed model analysis (summarised in Table 3) revealed significant between-condition differences at grand mean of stride duration for 22 out of the 31 outcome variables. Stride duration contributed significantly ($P \le 0.05$) in all models except the ones modelling Withers_Maxdiff, Neck_z_h2_amp, diag_diss (non-induced limb involvement) and lat_diss (induced limb involvement). The interaction between stride duration and condition was statistically significant ($P \le 0.05$), and therefore included, in 17 out of 31 models. Stride duration did not differ

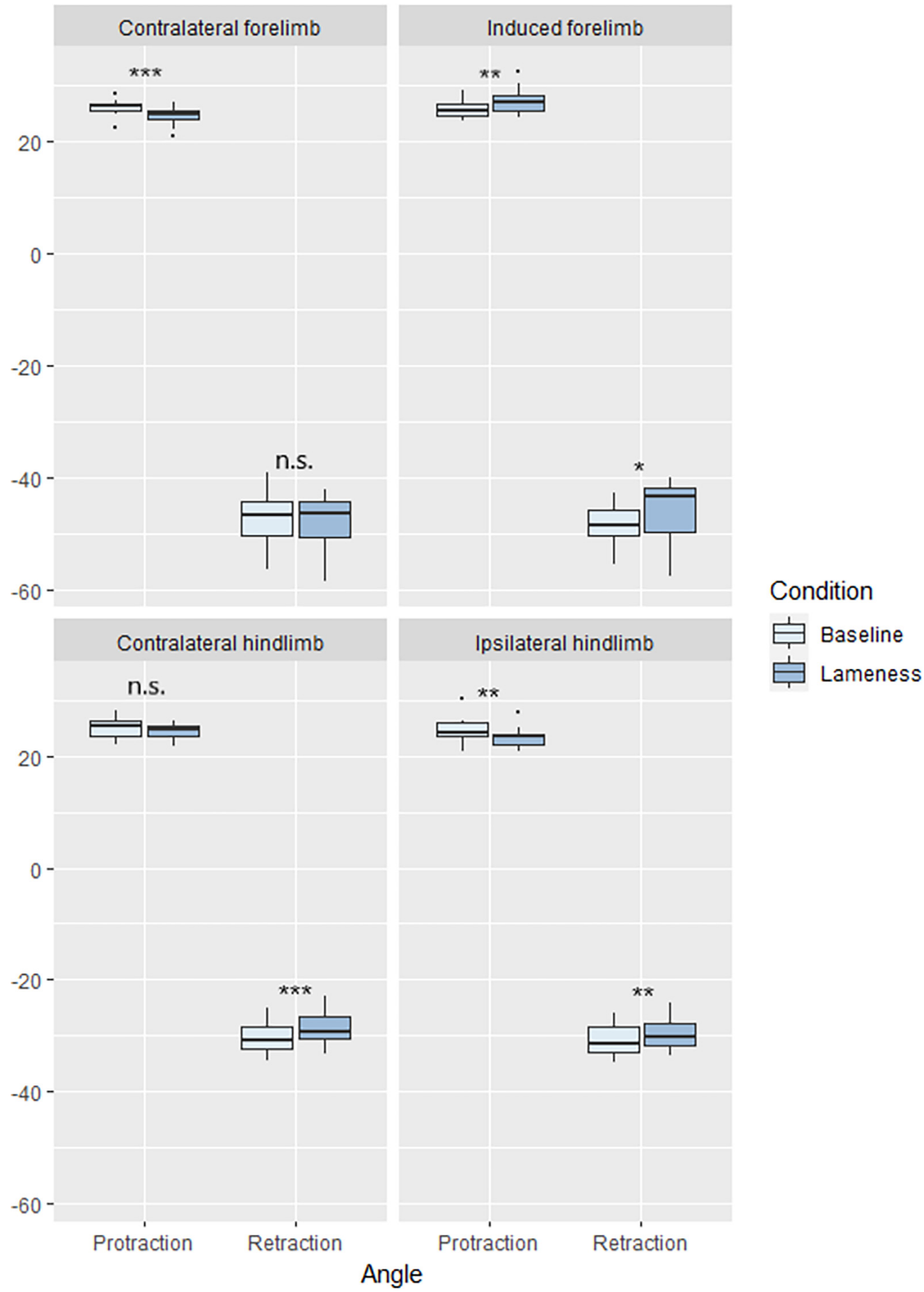

Fig. 5. Distribution of maximum protraction and retraction angles in degrees (averaged over each cow and condition) of each limb, in the baseline compared to the lameness condition. ***$P < 0.001$, **$P < 0.01$, *$P \leq 0.05$, n.s. = not significant.

significantly between conditions; the estimated marginal mean was 1.27 and 1.28 s for baseline and lameness condition respectively, $P = 0.30$.

Limb parameters

At grand mean stride duration, significant (all $P \leq 0.05$) absolute value decreases of the maximum retraction angle of the induced forelimb (re_max_induced_fore, −3.0°), the hindlimb of the non-induced side (re_max_non_induced_hind, −1.4°), and of the hindlimb of the induced side (re_max_induced_hind, −1.2°) were seen in the lameness condition compared to the baseline condition. There were also decreases in the maximum protraction angle of the non-induced forelimb (pro_noninduced_fore, −1.7°) and of the hindlimb on the same side as the induced forelimb (pro_induced_side_hind, −1.2°). The maximum protraction angle of the induced forelimb (pro_induced_fore) instead increased by 1.5° ($P \leq 0.05$). No changes were detected in the retraction angle of the non-induced forelimb ($P = 0.79$) or the protraction angle of the hindlimb of the non-induced side ($P = 0.15$) (Fig. 5).

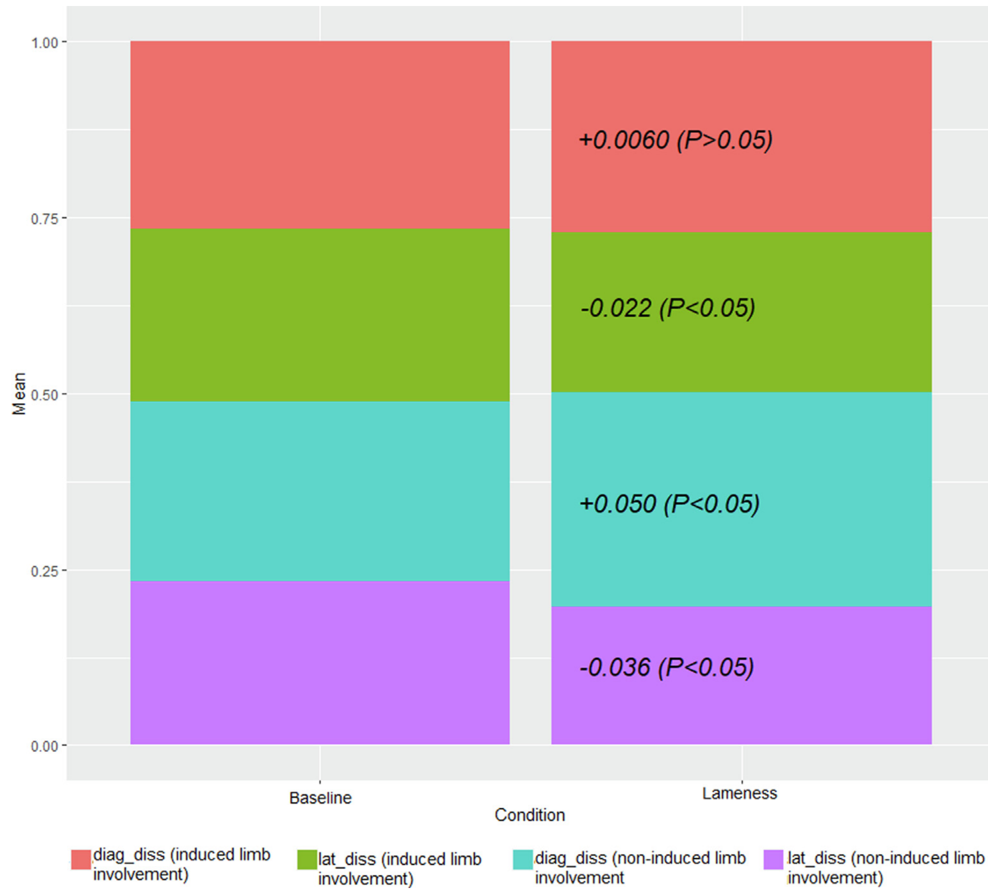

Fig. 6. Bar plots displaying average of temporal limb parameters (diag_diss = diagonal dissociation and lat_diss = lateral dissocitation), first averaged over each cow and then over each parameter, in the baseline compared to the lameness condition (N = 2 180 strides). For the lameness condition, model estimate differences compared to the baseline condition are indicated. As all temporal parameters were calculated on a stride-by-stride basis and expressed as a ratio of stride duration, both bars sum to one. Lat_diss (induced limb involvement) and lat_diss (non-induced limb involvement) decreased significantly, and diag_diss (non-induced limb involvement) increased significantly in the lameness compared to the baseline condition (all $P \leq 0.05$, linear mixed models). There was no significant difference in diag_diss (induced limb involvement) between the two conditions ($P = 0.26$, linear mixed model). All comparisons were executed at grand mean stride duration.

Differences between conditions (at grand mean stride duration) were also detected in three out of four investigated temporal parameters, as visualised in Fig. 6. The relative time between hoof-on of the non-induced forelimb and its contralateral hindlimb (diag_diss, non-induced limb involvement) increased by 0.050 (ratio of stride duration). The relative time between the hoof-on moments of the hindlimb ipsilateral to the induced forelimb and the induced forelimb (lat_diss, induced limb involvement) decreased by 0.022, and the time between the hoof-on moments of the hindlimb ipsilateral to the non-induced forelimb and the non-induced forelimb (lat_diss, non-induced limb involvement) decreased by 0.036 (all $P \leq 0.05$). Diag_diss (induced limb involvement) did not change ($P = 0.26$).

Upper body parameters

The vertical range of motion increased (all $P \leq 0.05$, at grand mean stride duration) during lameness for the poll, neck and back IMUs, and decreased for the TS IMU. For the withers IMU, this parameter did not change ($P = 0.77$). For the poll and neck IMUs, there was clear evidence of increased within-stride vertical displacement asymmetry during lameness. More specifically, the amplitude of the first harmonic (expressed as a ratio of the total range of motion) of vertical displacement increased by 0.13 and 0.11 respectively, while the amplitude of the second harmonic of vertical displacement decreased by 0.10 and 0.05 respectively (all $P \leq 0.05$). Examples of vertical displacement for the poll IMU are shown in Fig. 7. Similarly, for the withers and TS IMUs, the amplitude of the second harmonic decreased (withers IMU: 0.04 decrease; TS IMU: 0.06 decrease, both $P \leq 0.05$), however, the first harmonic's amplitude did not change (withers IMU: $P = 0.087$; TS IMU: $P = 0.16$). For the back IMU, by contrast, the second harmonic amplitude increased with lameness induction (0.04 increase, $P \leq 0.05$), while the first harmonic amplitude remained unchanged ($P = 0.46$). Hence, for this IMU, no signs of increased within-stride vertical asymmetry were seen in the lameness condition. The distributions of the first and second harmonics' amplitudes for all upper body landmarks are visualised in Fig. 8.

The estimates for withers_Maxdiff and withers_Mindiff (visualised in Fig. 9) indicate slightly higher within-stride asymmetry of vertical displacement in the baseline compared to the lameness condition; the absolute values for these parameters were slightly higher prior to lameness induction than after. In the baseline condition, the withers' position was on average 5.43 mm higher during early stance of the (to be) induced forelimb compared to early stance of its contralateral forelimb. In the lameness condition, this situation was reversed; the position of the withers was instead, on average, 3.40 mm lower during early stance of the induced limb compared to early stance of the non-induced limb. Thus, in absolute values, this parameter changed by 8.83 mm ($P \leq 0.05$). For withers_Maxdiff, the absolute difference between the baseline and lameness conditions was smaller (3.99 mm, $P \leq 0.05$); at baseline, the withers' position was on average 2.41 mm higher during

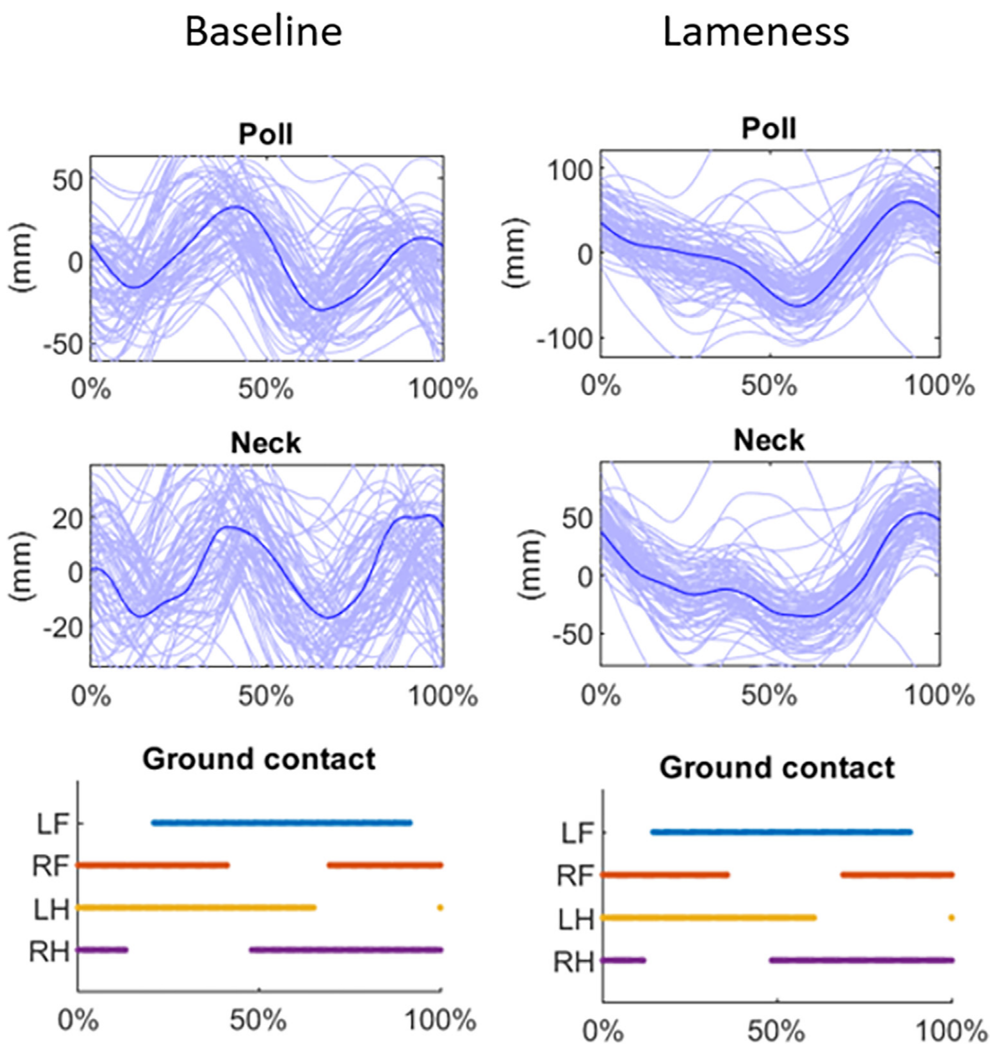

Fig. 7. Representative examples of vertical displacement in millimetres of the poll and neck IMUs. Baseline or lameness is indicated at the top of each column. The included plots are from cow 12, which had lameness induced on the right forelimb. Each stride is plotted as a light blue line, and the most common stride is plotted as a dark blue line. The Y-axis scale was set individually for each IMU (inertial measurement unit) and trial. All strides were time normalised, starting at 0% and ending at 100% of stride duration (indicated at the bottom of each sub-plot). Stance phases (mean across all strides for each trial) are shown in the bottom sub-plots; LF = left fore, RF = right fore, LH = left hind, RH = right hind. For both the poll and neck, a significant increase in the first harmonic amplitude and decrease in the second harmonic amplitude were seen, implying increased within-stride asymmetry. From the plots, it can (correspondingly) be seen that during lameness, the double-wave pattern seen at baseline is disrupted, and has moved towards a single-wave appearance. Hence, during lameness, the first rather than the second harmonic is dominating. Further, during lameness, the head-neck segment is carried at a lower position during stance of the non-lame limb (LF), and at a higher position during stance of the lame limb (RF). Vertical displacement plots for all upper body IMUs and trials can be found in Supplementary Fig. S1.

midstance of the (to be) induced limb, whereas the withers' position was on average 1.58 mm higher during midstance of the non-induced limb after induction. No changes in TS_Mindiff (P = 0.73) or TS_Maxdiff (P = 0.26) were detected. Examples of vertical displacement curves for the withers IMU are shown in Fig. 10. Vertical displacement curves for all upper body IMUs and trials are shown in Supplementary Fig. S1.

Discussion

This is, to the authors' best knowledge, the first study dedicated to investigating kinematic changes in dairy cows with forelimb lameness. Using a newly developed lameness induction method tailored to bovines, and a within-subjects study design where each cow acted as its own control, we were able to measure subtle kinematic changes associated with low-degree forelimb lameness in dairy cows. The study design where IMUs were used further enabled us to collect large amounts of data (> 25 stride cycles per trial) in comparison with previous studies on bovine lameness (Nejati et al., 2023). This is of importance to obtain high-quality data; the presence of considerable inter-stride variation of kinematic parameters has been reported previously by Telezhenko (2009), who further concluded that it is beneficial to use data from several stride cycles in order to obtain representative information on movement patterns.

Lameness induction had effects on limb maximum protraction and retraction (i.e., forward and backward extension) angles as well as on the inter-limb coordination pattern, as previously found in cows with induced hindlimb lameness (Leclercq et al., 2024); however, these parameters were altered differently during forelimb lameness. Forelimb lameness induction resulted in a small but significant increase in the maximum protraction angle of the induced (lame) limb, indicating a longer distance between the forelimbs during dual support with protraction of the induced limb. There were also small but significant decreases in the retraction angle of the induced limb, and the protraction angle of the non-

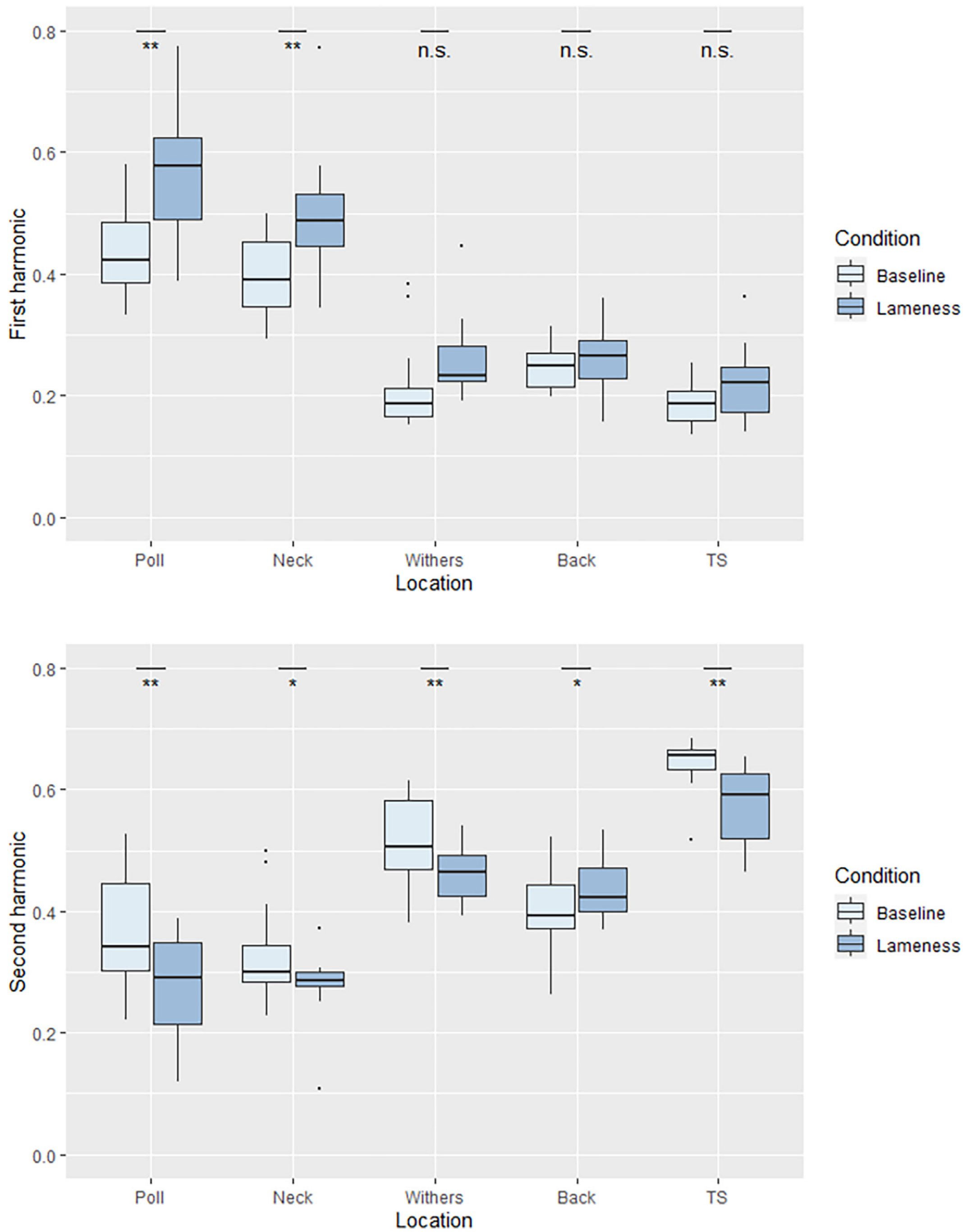

Fig. 8. Distributions of the amplitudes of the first (top panel) and second (bottom panel) harmonics of vertical displacement of all upper body IMU (inertial measurement unit) locations, in the baseline compared to the lameness condition. Boxplots were made from cow-level averages. $^*P \leq 0.05$, $^{**}P < 0.01$, n.s. = not significant. TS = *tubera sacrale*.

induced limb, instead indicating a shorter distance between the forelimbs during dual support with retraction of the induced limb. This may reflect the cow attempting to reduce the force acting on the induced forelimb by keeping it further away from the body's centre of mass (i.e. more cranially) throughout the stride cycle. This corresponds with findings in cows with hindlimb lameness, where the maximum protraction angle of the lame hindlimb instead decreased (Leclercq et al., 2024), i.e. the lame hindlimb was kept more caudally. Moreover, in the present study, all hindlimb protraction- and retraction angles except for the protraction angle of the hindlimb contralateral to the induced forelimb decreased, possibly reflecting a generally more "cautious" walk. At maximum protraction of the hindlimb contralateral to the induced forelimb, the induced forelimb would be approximately in midstance, i.e. subjected to large vertical forces (Van der Tol et al., 2003). Advancing its contralateral hindlimb relatively far in under the centre of mass might reduce (or avoid an increase of) the force to which the induced limb is subjected to during its midstance. Furthermore, during forelimb lameness, the cows' gait exhibited a more "pace-like" pattern compared to the baseline condition, as both forelimbs were (relative to stride duration) placed on the ground sooner after hoof-on of their respective ipsilateral hindlimb. Also, the relative time between hoof-on of the non-induced forelimb and hoof-on of its contralateral hindlimb

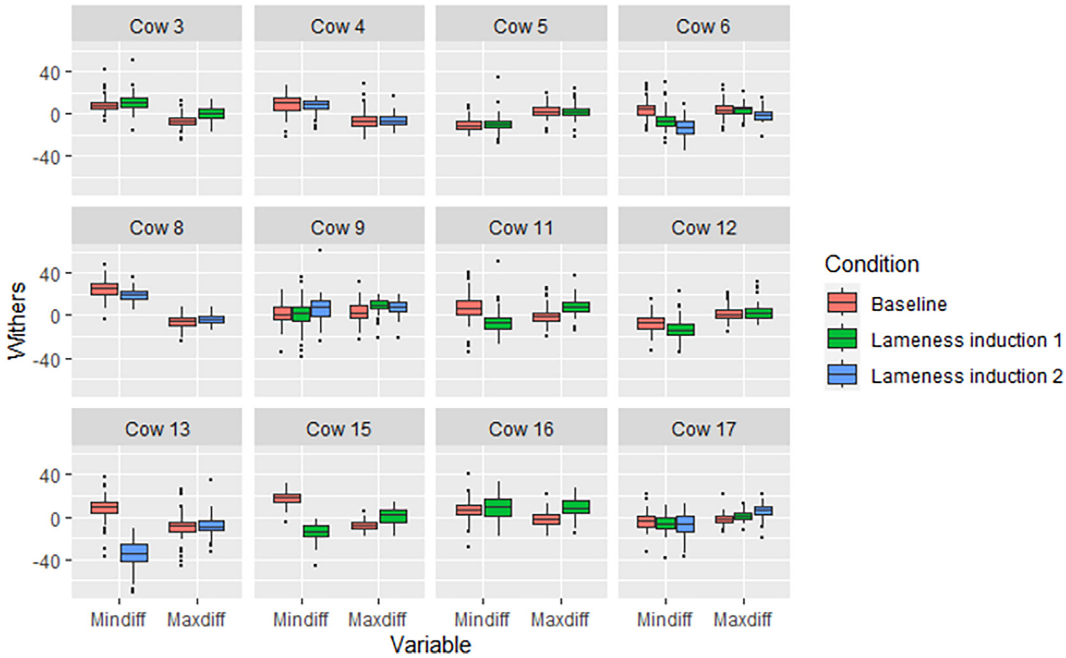

Fig. 9. Boxplots made from stride-by-stride data displaying the distribution of withers_Maxdiff and Withers_Mindiff in millimetres. Data were standardised to allow for group-level comparison. Cow ID (3–17) is indicated in each subplot. Linear mixed model analysis revealed significant changes in withers_Maxdiff and withers_Mindiff (both $P \leq 0.05$) in the lameness condition compared to the baseline condition. Comparisons were executed at grand mean stride duration. Maxdiff = within-stride difference between local maxima of vertical position in millimetres, Mindiff = within-stride difference between local minima of vertical position in millimetres.

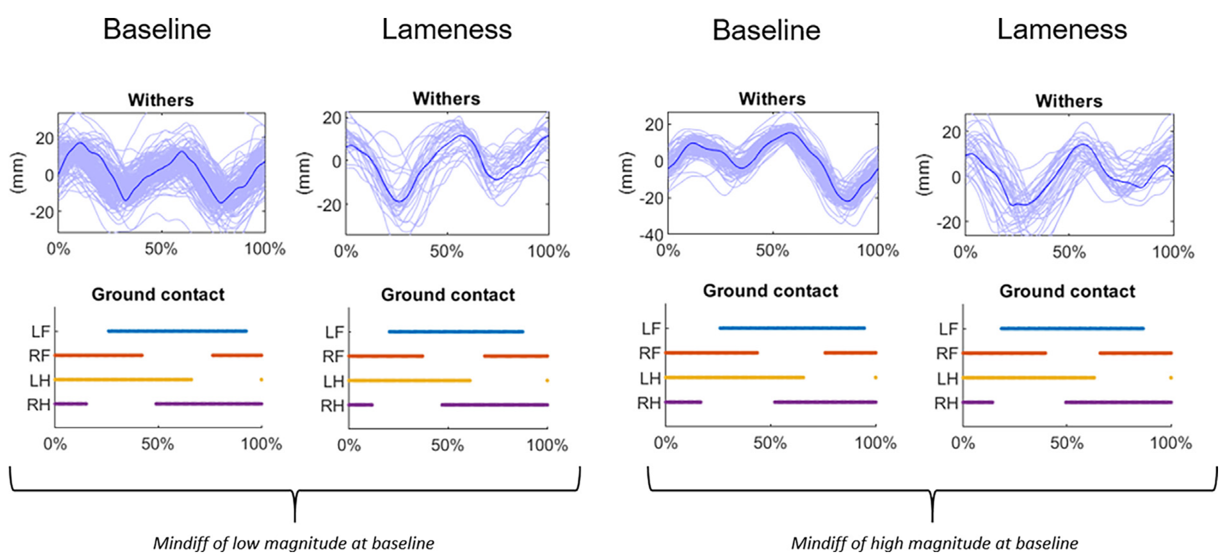

Fig. 10. Representative examples of vertical displacement in millimetres of the withers IMU (inertial measurement unit). Baseline or lameness is indicated at the top of each column. The included plots are from cow 15 (left) and cow 6 (right), which both had lameness induced on their left forelimb. Each stride is plotted as a light blue line, and the most common stride is plotted as a dark blue line. All strides were time normalised, starting at 0% and ending at 100% of stride duration (indicated at the bottom of each sub-plot). Stance phases (mean across all strides for each trial) are shown in the bottom sub-plots; LF = left fore, RF = right fore, LH = left hind, RH = right hind. For cow 15 (left), a very small difference between the two local minima is seen at baseline (i.e. withers_Mindiff is of low magnitude). During lameness, the difference becomes bigger. For cow 6 (right), a larger difference between the two local minima is seen at baseline (i.e. withers_Mindiff is of higher magnitude). During lameness, the absolute difference is smaller. However, a common pattern where the position of the withers was relatively lower during early stance of the induced (lame) limb, i.e. LF, in the lameness compared to the baseline condition is seen (demonstrated as an 8.83 mm change in withers_Mindiff). Vertical displacement plots for all upper body IMUs and trials can be found in Supplementary Fig. S1.

increased, while the relative time between hoof-on of the induced forelimb and its contralateral hindlimb did not change. These changes could translate to an "uneven temporal rhythm between hoof beats", which has previously been described as a visual lameness sign (Welfare Quality Network, 2023).

Lameness induction also caused kinematic changes in the upper body. For the poll and neck, large increases of the first harmonic relative amplitudes and decreases of the second harmonic relative amplitudes were seen. In other words, this indicates increased between stride-half differences in the up- and downward excursions of the head and neck during lameness. The vertical ranges of motion per stride of the poll and neck, respectively, also increased. Hence, the distance between the minimum and maximum vertical position within one stride was (on average) larger during lameness. Similar changes (i.e. increased movement asymmetry and range of motion of the head and neck) were also seen in cows with induced hindlimb lameness (Leclercq et al., 2024).

In coherence with the indications of increased within-stride vertical asymmetry, the vertical displacement plots (Fig. 7) show that during lameness, a single-wave pattern, rather than a double-wave pattern (which may be expected in sound animals) is common, as also reported in horses by Rhodin et al. (2016). Hence, the first rather than the second harmonic dominates in the lameness condition. This corresponds with "head bobbing", which is seen as an important visual sign of lameness and used in some existing subjective scoring systems (O'Callaghan et al., 2003; Flower and Weary, 2006). In the current study, it does moreover seem like the head and neck-segment is (relatively seen) lifted during stance of the induced forelimb and lowered during stance of the non-induced forelimb. Altering the movement of the head and neck in this way likely contributes to reducing the force acting on the painful limb during its stance phase.

For the withers, the changes in harmonic relative amplitudes were smaller, and a double-wave pattern of the vertical displacement is generally visible both in the baseline and in the lameness condition (examples shown in Fig. 10). While the relative amplitude of the first harmonic did not change with lameness induction, there was a significant decrease of the second harmonic relative amplitude. Although this partly indicates increased within-stride asymmetry during lameness, both withers_Mindiff and withers_Maxdiff do, by contrast, point towards slightly higher asymmetry in the baseline condition, where they are of higher magnitudes compared to the lameness condition. This stands in contrast to previous findings in walking cows (Leclercq et al., 2024), and to the general perception that lameness is associated with increased movement asymmetry. However, withers movement asymmetry has also been reported in sound, walking horses (Byström et al., 2018). It should be noted that baseline values vary between individuals (see Fig. 9); however, even though "starting values" differ between cows, systematic patterns can be discerned, demonstrated as significant changes both in withers_Mindiff and withers_Maxdiff. For withers_Mindiff, the estimate is positive in the baseline condition but becomes negative during lameness, indicating that the withers on average came to a lower position during protraction of the induced forelimb compared to the non-induced forelimb, relative to the baseline condition. This seems logical in relation to the changes in the distal forelimb angles, which indicated an increased limb spread during dual forelimb support with protraction of the induced limb, and a reduced limb spread during dual support with protraction of the non-induced limb.

Based on the above, one may also reflect upon methodological choices, and what strategy might be best to assess upper body vertical symmetry in walking bovines. As opposed to harmonic amplitudes, Mindiff and Maxdiff (i.e. within-stride differences between peaks and troughs) are calculated directly from the vertical displacement signal, and thus components of higher frequencies (3rd harmonic and above) might have contributed to variability in data, and to the somewhat unexpected results (that is, indications of higher degree of asymmetry in the baseline compared to the lameness condition). In other words, it may be that the first and second harmonics provide "cleaner" information regarding an animal's lameness status than calculations of upper body kinematic parameters from the original signal. Signal decomposition methods might be a better strategy as analyses can be based on extracted components deemed relevant to explain the motion, while potentially "disturbing" higher-frequency components are not considered. However, calculations of within-stride extreme value differences between peaks and troughs based on the original vertical displacement signal are advantageous as it can indicate whether the asymmetry occurred during midstance (Maxdiff), during limb spread (Mindiff), and during the left or right limb step (indicated by positive/negative signs). Thereby, these measures can potentially indicate the limb which is lame. Analysis of harmonic amplitudes provides more unspecific information, where only the magnitude of vertical asymmetry, and not which part of the stride cycle the asymmetry occurred, is considered. In the future, one way to quantify movement asymmetry while also being able to determine in which part(s) of the stride cycle it occurs may hence be to use the amplitudes of the first and second harmonics, as well as their phase angles. Either way, "normal" or "baseline" values are likely to vary (Tijssen et al., 2021), and to be able to detect low-degree lameness, each cow is likely to serve best as its own reference. In other words, clinically sound animals should not be expected to exhibit completely symmetrical movement patterns, and it is not recommended to apply set thresholds on a herd level to differ between mildly lame and non-lame animals.

For the pelvis (TS IMU), a significantly decreased vertical range of motion was seen during lameness. This seems logic as decreases in maximum distal hindlimb angles (indicating shorter distance between the hindlimbs during limb spread, which should affect the position of the pelvis) were also seen. In hindlimb lame cows, on the contrary, this parameter increased (Leclercq et al., 2024), indicating that also pelvis kinematic changes differ between fore- and hindlimb lameness. Similarly, as for the withers, the relative amplitude of the second harmonic of the *tuber sacrales'* vertical displacement decreased significantly during lameness while the first harmonic amplitude remained unchanged. For TS_Mindiff and TS_Maxdiff, however, the estimates were close to zero, indicating almost complete symmetry on a group level, in both conditions. One possible explanation to these somewhat contradictory results is that as mentioned, the amplitudes of harmonic waves do not provide any information regarding the part(s) of the stride cycle in which the asymmetry occurred, as opposed to Maxdiff and Mindiff. Hence, when computing Mindiff and Maxdiff, inter-individual variability regarding which part(s) of the stride cycle was affected by lameness induction can cause variability in data, and group-level patterns will not be discernible. In other words, it might be that pelvis vertical asymmetry is altered in different ways depending on the individual. Therefore, pelvis vertical asymmetry parameters may not be a reliable indicator of mild forelimb lameness in cows.

For the back IMU, a significant increase in the vertical range of motion per stride was seen in the lameness condition, as also reported in cows with induced hindlimb lameness (Leclercq et al., 2024). This may be perceived as if the back is arching during locomotion, which is one of the most important gait features assessed in the Sprecher lameness scale (Sprecher et al., 1997). When it comes to the relative amplitudes of the first and second harmonics of vertical displacement, there was a significant increase in the second harmonic amplitude in the lameness condition, while the first harmonic amplitude remained unchanged on a group level. Hence, no evidence of increased movement asymmetry of the back was found. This stands in contrast with findings from cows with induced hindlimb lameness, where vertical movement asymmetry clearly increased in lame animals (Leclercq et al., 2024). In the current study, the results rather indicate an increase in the range of motion which seems to be largely explained by an increase in the second harmonic (i.e. the symmetric component of the motion). Hence, while an increased vertical range of motion by itself could indicate mild forelimb lameness, an increased range of motion together with increased vertical asymmetry could indicate hindlimb lameness (Leclercq et al., 2024). This further underscores that these two conditions are associated with different movement patterns, thus showing potential for the development of surveillance systems which are able to differentiate between the two.

To summarise, lameness induction resulted in altered interlimb coordination, where the walking gait became more "pace-like" in the lameness condition. There were small but significant changes in distal limb angles, indicating increased limb spread during protraction of the induced limb, and decreased limb spread during protraction of its counterpart, where the position of the withers was altered accordingly. For the poll and neck, distinct increases in within-stride vertical symmetry, as well as range of motion, were seen. The vertical range of motion of the back increased, while it decreased for the TS. Many of the observed changes were, though systematic, subtle, reflecting the low degree of lameness studied here, and are therefore not likely to be detectable through visual assessment alone. For the same reason, they might not be very informative if considered individually. Instead, to improve early-stage lameness detection, it is likely of importance to obtain information from numerous body locations, using objective methods which are able to recognise characteristic movement patterns associated with mild fore- and hindlimb lameness respectively. In the future, machine learning approaches could further be of interest to more precisely define which parameters this "pattern" should be consisted of to be able to discriminate between lame and sound animals as accurately and efficiently as possible.

In this study, a newly developed method for mechanical lameness induction was used. Although not commonly used in bovine research, mechanical lameness induction methods have frequently been employed in studies investigating lameness in equines (e.g. Weishaupt et al., 2004, 2006; Rhodin et al., 2018). In previous studies on lameness in bovines, visual lameness assessment has often served as the only reference method (i.e., as the "ground truth") (Alsaaod et al., 2019; Afonso et al., 2020) which represents a major limitation because of the inherent subjectivity of visual lameness assessment. When lameness induction methods are used, within-subject study designs can conveniently be employed, which is advantageous when aiming to capture small fluctuations in kinematics while accounting for inter-individual differences, as is likely necessary to be able to develop systems which can detect early-stage lameness. Nevertheless, although the induction methods used were developed to mimic common claw pathologies, and caused a movement pattern which was visually very similar to the one seen during clinical lameness, follow-up studies on clinically lame cows are needed to confirm results in "real-life" conditions. Despite the perceived similarity, the movement pattern observed during induced lameness may differ from that seen in clinical lameness, where e.g. lesion type and chronicity may vary, which could potentially influence results. Longitudinal studies are also warranted to investigate the within-individual stability of the studied parameters over time and through different lameness episodes.

Conclusion

In conclusion, this study identified several potentially useful kinematic parameters for the detection of forelimb lameness in dairy cows, related both to the limbs and to the upper body. We also showed that for many parameters, fore- and hindlimb lameness are associated with different kinematic changes (Leclercq et al., 2024). Furthermore, the advantages of using each individual as its own control when attempting to measure subtle kinematic changes associated with mild lameness were accentuated. While the IMU–based data collection methods used here are far too impractical to implement directly on commercial farms, our results can contribute to the further development of video-based lameness detection tools, as well as further development of signal processing approaches. Considering recent advancements in computer vision (Anagnostopoulos et al., 2023; Järemo Lawin et al., 2023; Russello et al., 2022; 2024), marker-less gait analysis tools capable of monitoring kinematics of numerous anatomical locations simultaneously may soon be common in farms. This could enable detection of specific, lameness-related changes in the overall movement pattern, facilitating early diagnosis of mild lameness cases.

Supplementary material

Supplementary Material for this article (https://doi.org/10.1016/j.animal.2025.101482) can be found at the foot of the online page, in the Appendix section.

Ethics approval

This study was approved by the Swedish Ethics Committee and performed according to the Swedish legislation on animal experiments (diary number 5.8.18-10570/2019). The 3 Rs (Reduce, Refine, Replace) were considered during planning and execution of the study.

Data and model availability statement

None of the data were deposited in an official repository, but they are available upon request to the authors.

Declaration of Generative AI and AI-assisted technologies in the writing process

During the preparation of this work the author(s) did not use any AI and AI-assisted technologies.

Author ORCIDs

Anna Leclercq: https://orcid.org/0000-0002-7108-9781.
Katrina Ask: https://orcid.org/0000-0002-7336-3852.
Ylva Mellbin: https://orcid.org/0009-0006-8801-343X.
Anna Byström: https://orcid.org/0000-0002-2008-8244.
Maja Söderlind: https://orcid.org/0009-0001-1548-1711.
Evgenij Telezhenko: https://orcid.org/0000-0001-7388-8205.
Christer Bergsten: https://orcid.org/0000-0003-0901-4698.
Pia Haubro Andersen: https://orcid.org/0000-0002-6039-7439.
Marie Rhodin: https://orcid.org/0000-0003-0575-2765.
Elin Hernlund: https://orcid.org/0000-0002-5769-3958.

CRediT authorship contribution statement

A. Leclercq: Writing – review & editing, Writing – original draft, Visualisation, Validation, Methodology, Formal analysis, Data curation. **K. Ask:** Writing – review & editing, Methodology, Investigation, Data curation. **Y. Mellbin:** Writing – review & editing, Visualisation, Software, Formal analysis. **A. Byström:** Writing – review & editing, Software, Methodology, Formal analysis. **M. Söderlind:** Writing – review & editing, Data curation. **E. Telezhenko:** Writing – review & editing, Methodology, Investigation. **C. Bergsten:** Writing – review & editing, Methodology, Investigation. **P. Haubro Andersen:** Writing – review & editing, Funding acquisition, Conceptualisation. **M. Rhodin:** Writing – review & editing, Supervision, Resources, Funding acquisition, Conceptualisation. **E. Hernlund:** Writing – review & editing, Supervision, Resources, Funding acquisition, Conceptualisation.

Declaration of interest

None.

Acknowledgements

We would like to thank the staff and animals at the Swedish Livestock Research Centre at Lövsta, Swedish University of Agricultural Science, for their contributions. We also want to thank J. Lundblad, C. Frisk and M. Tijssen for their help during data collection.

Financial support statement

This work was supported by the Swedish Research Council FORMAS (grant number 2016-01760), and by the Beijer Foundation.

References

Afonso, J.S., Bruce, M., Keating, P., Raboisson, D., Clough, H., Oikonomou, G., Rushton, J., 2020. Profiling detection and classification of lameness methods in british dairy cattle research: a systematic review and meta-analysis. Frontiers in Veterinary Science 7, 542.

Alsaaod, M., Fadul, M., Steiner, A., 2019. Automatic lameness detection in cattle. The Veterinary Journal 246, 35–44.

Anagnostopoulos, A., Griffiths, B.E., Siachos, N., Neary, J., Smith, R.F., Oikonomou, G., 2023. Initial validation of an intelligent video surveillance system for automatic detection of dairy cattle lameness. Frontiers in Veterinary Science 10, 1111057.

Audigié, F., Pourcelot, P., Degueurce, C., Geiger, D., Denoix, J.M., 2002. Fourier analysis of trunk displacements: a method to identify the lame limb in trotting horses. Journal of Biomechanics 35, 1173–1182.

Bates, D., Mächler, M., Bolker, B., Walker, S., 2015. Fitting linear mixed-effects models using lme4. Journal of Statistical Software 67, 1–48.

Bosch, S., Serra Bragança, F., Marin-Perianu, M., Marin-Perianu, R., van der Zwaag, B. J., Voskamp, J., Back, W., van Weeren, R., Havinga, P., 2018. EquiMoves: a wireless networked inertial measurement system for objective examination of horse gait. Sensors 18, 850.

Buchner, H.H.F., Savelberg, H.H.C.M., Schamhardtt, H.C., Barneveld, A., 1996. Head and trunk movement adaptations in horses with experimentally induced fore- or hindlimb lameness. Equine Veterinary Journal 28, 71–76.

Byström, A., Egenvall, A., Roepstorff, L., Rhodin, M., Serra Bragança, F., Hernlund, E., Van Weeren, R., Weishaupt, M.A., Clayton, H.M., 2018. Biomechanical findings in horses showing asymmetrical vertical excursions of the withers at walk. PLoS One 13, e0204548.

Cha, E., Hertl, J.A., Bar, D., Gröhn, Y.T., 2010. The cost of different types of lameness in dairy cows calculated by dynamic programming. Preventive Veterinary Medicine 97, 1–8.

Coetzee, J.F., Mosher, R.A., Anderson, D.E., Robert, B., Kohake, L.E., Gehring, R., White, B.J., KuKanich, B., Wang, C., 2014. Impact of oral meloxicam administered alone or in combination with gabapentin on experimentally induced lameness in beef calves. Journal of Animal Science 92, 816–829.

Cramer, G., Solano, L., 2023. Interdigital Hyperplasia in Cattle. Retrieved on 27 January 2025 from: https://www.msdvetmanual.com/musculoskeletal-system/lameness-in-cattle/lameness-originating-in-the-hoof-in-cattle#Interdigital-Hyperplasia_v80036517.

Croyle, S., Belage, E., Khosa, D., Leblanc, S.J., Haley, D.B., Kelton, D.F., 2019. Dairy farmers' expectations and receptivity regarding animal welfare advice: a focus group study. Journal of Dairy Science 102, 7385–7397.

Fabian, J., Laven, R.A., Whay, H.R., 2014. The prevalence of lameness on New Zealand dairy farms: a comparison of farmer estimate and locomotion scoring. Veterinary Journal 201, 31–38.

Fenster, L.L., Ruchti, L.L., Credille, B.C., 2023. Retrospective evaluation of the causes and distribution of lameness in beef and dairy cattle evaluated by ambulatory and in-house clinical services at a North American veterinary teaching hospital. Journal of the American Veterinary Medical Association 261, 989–994.

Flower, F., Weary, D., 2006. Effect of hoof pathologies on subjective assessments of dairy cow gait. Journal of Dairy Science 89, 139–146.

Fox, J., Weisberg, S., 2019. An R companion to applied regression. Sage, Thousand Oaks, CA, USA.

Halekoh, U., Højsgaard, S., 2014. A Kenward-Roger approximation and parametric bootstrap methods for tests in linear mixed models – the R package pbkrtest. Journal of Statistical Software 59, 1–30.

Jaja, I.F., Yanga, D.S., 2022. Culling and mortality of dairy cows: why it happens and how it can be mitigated. F1000Research 10, 1014.

Järemo Lawin, F., Byström, A., Roepstorff, C., Almlöf, M., Silva, M., Rhodin, M., Haubro Andersen, P., Kjellström, H., Hernlund, E., 2023. Is markerless more or less? Comparing a smartphone computer vision method for equine lameness assessment to multi camera motion capture. Animals 13, 390.

Jubb, T.F., Malmo, J., 1991. Lesions causing lameness requiring veterinary treatment in pasture-fed dairy cows in East Gippsland. Australian Veterinary Journal 68, 21–24.

Kaneps, A.J., 2014. Diagnosis of lameness. In: Hinchcliff, K.W., Kaneps, A.J., Geor, R.J. (Eds.), Equine Sports Medicine and Surgery. Second Ed. Saunders, Philadelphia, PA, USA, pp. 239–251.

Keegan, K.G., Pai, P.F., Wilson, D.A., Smith, B.K., 2001. Signal decomposition method of evaluating head movement to measure induced forelimb lameness in horses trotting on a treadmill. Equine Veterinary Journal 33, 446–451.

Kuznetsova, A., Brockhoff, P.B., Christensen, R.H.B., 2017. lmerTest package: tests in linear mixed effects models. Journal of Statistical Software 82, 1–26.

Leach, K.A., Whay, H.R., Maggs, C.M., Barker, Z.E., Paul, E.S., Bell, A.K., Main, D.C.J., 2010. Working towards a reduction in cattle lameness: 1. Understanding barriers to lameness control on dairy farms. Research in Veterinary Science 89, 311–317.

Leach, K.A., Tisdall, D.A., Bell, N.J., Main, D.C.J., Green, L.E., 2012. The effects of early treatment for hindlimb lameness in dairy cows on four commercial UK farms. The Veterinary Journal 193, 626–632.

Leclercq, A., Ask, K., Byström, A., Mellbin, Y., Serra Bragança, F., Telezhenko, E., Bergsten, C., Söderlind, M., Haubro Andersen, P., Rhodin, M., Hernlund, E., 2024. Kinematic changes in dairy cows with induced hindlimb lameness: transferring methodology from the field of equine biomechanics. Animal 18, 101269.

Lenth, R., 2023. emmeans: Estimated Marginal Means, aka Least-Squares Means. R package version 1.9. Retrieved in 2023 from: https://CRAN.R-project.org/package=emmeans.

Lischer, C.J., Ossent, P., Räber, M., Geyer, H., 2002. Suspensory structures and supporting tissues of the third phalanx of cows and their relevance to the development of typical sole ulcers (Rusterholz ulcers). Veterinary Record 151, 694–698.

Loscher, D.M., Meyer, F., Kracht, K., Nyakatura, J.A., 2016. Timing of head movements is consistent with energy minimization in walking ungulates. Proceedings of the Royal Society B: Biological Sciences 283, 20161908.

Manske, T., Hultgren, J., Bergsten, C., 2002. Prevalence and interrelationships of hoof lesions and lameness in Swedish dairy cows. Preventive Veterinary Medicine 54, 247–263.

Nejati, A., Bradtmueller, A., Shepley, E., Vasseur, E., 2023. Technology applications in bovine gait analysis: a scoping review. PLoS One 18, e0266287.

O'Callaghan, K.A., Cripps, P.J., Downham, D.Y., Murray, R.D., 2003. Subjective and objective assessment of pain and discomfort due to lameness in dairy cattle. Animal Welfare 12, 605–610.

O'Connor, A.H., Shalloo, L., Bokkers, E., de Boer, I., Hogeveen, H., Sayers, R., Byrne, N., Ruelle, E., 2023. Modeling the economic impacts of mobility scores in dairy cows under Irish spring pasture-based management. Journal of Dairy Science 106, 1218–1232.

Peham, C., Scheidl, L., Licka, T., 1996. A method of signal processing in motion analysis of the trotting horse. Journal of Biomechanics 29, 1111–1114.

Persson-Sjodin, E., Hernlund, E., Pfau, T., Andersen, P.H., Forsström, K.H., Byström, A., Serra Bragança, F.M., Hardeman, A., Greve, L., Egenvall, A., Rhodin, M., 2023. Withers vertical movement symmetry is useful for locating the primary lame limb in naturally occurring lameness. Equine Veterinary Journal 56, 76–88.

Pfau, T., Witte, T.H., Wilson, A.M., 2005. A method for deriving displacement data during cyclical movement using an inertial sensor. Journal of Experimental Biology 208, 2503–2514.

R Core Team, 2023. R: A Language and Environment for Statistical Computing. R Foundation for Statistical Computing, Vienna, Austria. Retrieved on 31 March 2025 from: https://www.R-project.org/.

Rhodin, M., Serra Bragança, F.M., Persson-Sjodin, E., Roepstorff, L., Weishaupt, M.A., Egenvall, A., Pfau, T., 2016. Lack of a Double-Peaked Vertical Head Movement in Moderately Lame Horses with Induced Lameness. Proceedings of the 8th international conference on canine and equine locomotion, 17–19 August 2016, London, United Kingdom, p. 37.

Rhodin, M., Persson-Sjodin, E., Egenvall, A., Serra Bragança, F.M., Pfau, T., Roepstorff, L., Weishaupt, M.A., Thomsen, M.H., van Weeren, P.R., Hernlund, E., 2018. Vertical movement symmetry of the withers in horses with induced forelimb and hindlimb lameness at trot. Equine Veterinary Journal 50, 818–824.

Roepstorff, C., Dittmann, M.T., Arpagaus, S., Serra Bragança, F.M., Hardeman, A., Persson-Sjödin, E., Roepstorff, L., Gmel, A.I., Weishaupt, M.A., 2021. Reliable and clinically applicable gait event classification using upper body motion in walking and trotting horses. Journal of Biomechanics 114, 110146.

Russello, H., Van Der Tol, R., Kootstra, G., 2022. T-LEAP: Occlusion-robust pose estimation of walking cows using temporal information. Computers and Electronics in Agriculture 192, 106559.

Russello, H., Van Der Tol, R., Holzhauer, M., Van Henten, E.J., Kootstra, G., 2024. Video-based automatic lameness detection of dairy cows using pose estimation and multiple locomotion traits. Computers and Electronics in Agriculture 223, 109040.

Serra Bragança, F.M., Bosch, S., Voskamp, J.P., Marin-Perianu, M., Van der Zwaag, B.J., Vernooij, J.C.M., van Weeren, P.R., Back, W., 2017. Validation of distal limb mounted inertial measurement unit sensors for stride detection in Warmblood horses at walk and trot. Equine Veterinary Journal 49, 545–551.

Serra Bragança, F.M., Rhodin, M., van Weeren, P.R., 2018. On the brink of daily clinical application of objective gait analysis: what evidence do we have so far from studies using an induced lameness model? Veterinary Journal 234, 11–23.

Serra Bragança, F.M., Hernlund, E., Thomsen, M.H., Waldern, N.M., Rhodin, M., Byström, A., van Weeren, P.R., Weishaupt, M.A., 2021. Adaptation strategies of horses with induced forelimb lameness walking on a treadmill. Equine Veterinary Journal 53, 600–611.

Smit, I.H., Hernlund, E., Persson-Sjodin, E., Björnsdóttir, S., Gunnarsdottir, H., Gunnarsson, V., Rhodin, M., Serra Bragança, F.M., 2023. Adaptation strategies of the Icelandic horse with induced forelimb lameness at walk, trot and tölt. Equine Veterinary Journal 56, 617–630.
Sprecher, D.J., Hostetler, D.E., Kaneene, J.B., 1997. A lameness scoring system that uses posture and gait to predict dairy cattle reproductive performance. Theriogenology 47, 1179–1187.
Telezhenko, E., 2009. Measurement of spatial gait parameters from footprints of dairy cows. Animal 3, 1746–1753.
Thomas, A.D., Orsel, K., Cortés, J.A., Pajor, E.A., 2022. Objective determination and quantification of pain and inflammation associated with digital dermatitis in feedlot cattle. Applied Animal Behaviour Science 253, 105684.
Thomsen, P.T., Shearer, J.K., Houe, H., 2023. Prevalence of lameness in dairy cows: a literature review. The Veterinary Journal 295, 1090–10233.
Tijssen, M., Serra Bragança, F.M., Ask, K., Rhodin, M., Andersen, P.H., Telezhenko, E., Bergsten, C., Nielen, M., Hernlund, E., 2021. Kinematic gait characteristics of straight line walk in clinically sound dairy cows. PLoS One 16, e0253479.
Toussaint-Raven, E., Haalstra, R.T., Petersen, D.J., 1989. Cattle footcare and claw trimming. Farming Press, Ipswich, United Kingdom.
Valenti, R.G., Dryanovski, I., Xiao, J., 2015. Keeping a good attitude: a quaternion-based orientation Fil- ter for IMUs and MARGs. Sensors 15, 19302–19330.
Van Der Tol, P.P.J., Metz, J.H.M., Noordhuizen-Stassen, E.N., Back, W., Braam, C.R., Weijs, W.A., 2003. The vertical ground reaction force and the pressure distribution on the claws of dairy cows while walking on a flat substrate. Journal of Dairy Science 86, 2875–2883.
Van Metre, D.C., 2017. Pathogenesis and treatment of bovine foot rot. Veterinary Clinics of North America - Food Animal Practice 33, 183–194.
Ventura, B.A., von Keyserlingk, M.A.G., Weary, D.M., 2015. Animal welfare concerns and values of stakeholders within the dairy industry. Journal of Agricultural and Environmental Ethics 28, 109–126.
Walker, A.M., Pfau, T., Channon, A., Wilson, C., 2010. Assessment of dairy cow locomotion in a commercial farm setting: the effects of walking speed on ground reaction forces and temporal and linear stride characteristics. Research in Veterinary Science 88, 179–187.
Weishaupt, M.A., Wiestner, T., Hogg, H.P., Jordan, P., Auer, J.A., 2004. Compensatory load redistribution of horses with induced weightbearing hindlimb lameness trotting on a treadmill. Equine Veterinary Journal 36, 727–733.
Weishaupt, M.A., Wiestner, T., Hogg, H.P., Jordan, P., Auer, J.A., 2006. Compensatory load redistribution of horses with induced weight-bearing forelimb lameness trotting on a treadmill. The Veterinary Journal 171, 135–146.
Welfare Quality Network, 2023. Welfare Quality Assessment Protocol for dairy cows version 3.0. Retrieved on 14 January 2025 from: https://www.welfarequalitynetwork.net/en-us/reports/assessment-protocols.
Winckler, C., Willen, S., 2001. The reliability and repeatability of a lameness scoring system for use as an indicator of welfare in dairy cattle. Acta Agriculturae Scandinavica 30, 103–107.